AN INVESTIGATION INTO THE PRECURSOR STATES FOR THE GRAPHITIZATION OF PYRENE
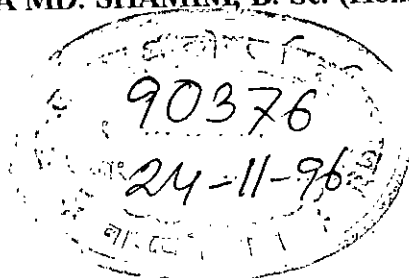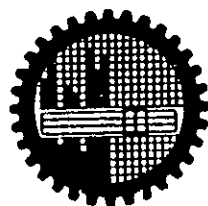
By

MIRZA MD. SHAMIM, B. Sc. (Hons.), M. Sc.

90376

24-11-96

A THESIS SUBMITTED TO THE DEPARTMENT OF PHYSICS,
BANGLADESH UNIVERSITY OF ENGINEERING & TECHNOLOGY IN
PARTIAL FULFILLMENT OF THE REQUIREMENT FOR THE DEGREE OF
MASTER OF PHILOSOPHY

BANGLADESH UNIVERSITY OF ENGINEERING & TECHNOLOGY, DHAKA,
BANGLADESH

DECLARATION

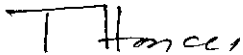*This thesis work has been done by the candidate himself and does not contain any material extracted from elsewhere or from a work published by any body else. The work of this thesis has not been presented by the candidate for any degree or diploma elsewhere. No other person's work has been used without due acknowledgment.*

10.9.96

(Mirza Md. Shamim)
Candidate
Roll No.: 9114F
Regd. No.: 89104
Session: 1989-90

CERTIFICATE

This is to certify that the research work embodying in this thesis has been carried out under my supervision. The research work presented herein is original. This thesis has not been submitted for the award of any other degree or diploma in any of the University.

(Prof. Dr. T. Hossain)
Supervisor
Dept. of Physics
Bangladesh University
of Engineering & Tech.
Dhaka, Bangladesh.

ACKNOWLEDGEMENT

BANGLADESH UNIVERSITY OF ENGINEERING AND TECHNOLOGY, DHAKA

DEPARTMENT OF PHYSICS

Certification of Thesis work

A Thesis on

AN INVESTIGATION INTO THE PRECURSOR STATES FOR THE GRAPHITIZATION OF PYRENE
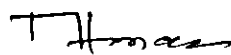
BY

Mirza Md. Shamim
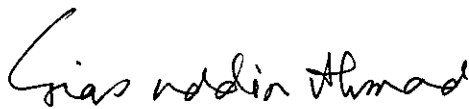
has been accepted as satisfactory in partial fulfilment for the degree of Master of Philosophy in Physics and certifying that the student demonstrated a satisfactory knowledge of the field covered by this thesis in an oral examination held on ....6.:....!!.:........ 1996.

Board of Examiners
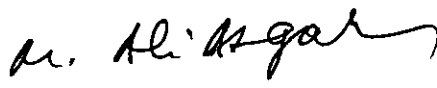
1. Dr. Tafazzal Hossian
    Professor of Physics
    BUET, Dhaka.   Supervisor & Chairman
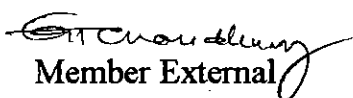
2. Dr. Gias uddin Ahmad
    Head & Professor of Physics
    BUET, Dhaka.   Member

3. Dr. M. Ali Asgar
    Professor of Physics
    BUET, Dhaka.   Member

4. Prof. Dr. M. G. Mowla Chowdhury
    Department of Physics
    University of Rajshahi
    Rajshahi   Member External

ABSTRACT

Pyrolysis of pyrene has been carried out to examine whether it is possible to produce condensed planar sheets of aromatic rings to form graphite and also to investigate whether the degree of graphitization relatively increases compared with other lower aromatic ring compounds or not. In the initial stages of nucleation and growth, a liquid-state mesophase of optical anisotropy appears as spherules in the sample. As carbonization progresses, the growing mesophase spherules change in shape in forming relatively complex bulk mesophase and mosaic texture. Reflected polarized-light micrography using cross polarizers with a gypsum plate at 45^0 with one of the polars [Sensitive Tint Technique] has been employed to investigate the microstructure of carbonaceous mesophase displaying maltese cross patterns and nodes as well as mosaic texture. Differential thermal analysis has been employed to locate the temperature region of mesophase formation. Thermogravimetric analysis has been used to see the quantitative analysis of the sample and to calculate the dynamic weight loss of the sample during carbonization. Interlayer spacing calculated from the X-ray diffractograms of the carbonized samples is found to decrease with heat-treatment temperature and duration. A comparative study has been carried out with the interlayer spacings of some lower aromatic compounds under similar condition. IR spectra have been used to substantiate the above results about the structural modifications of the carbonized samples. The broadening of the peak area of the aromatic band by IR study reveals about the order of the degree of graphitization.

LIST OF ABBREVIATIONS

BSU	*Basic Structural Unit*
DTA	*Differential Thermal Analysis*
E-ray	*Extra-ordinary ray*
HTT	*Heat-treatment temperature*
IR	*Infrared*
O-ray	*Ordinary ray*
PVC	*Polyvinyl Chloride*
PyC	*Pyrolytic Carbon*
TGA	*Thermogravimetric Analysis*
XRD	*X-ray Diffractometry*

CONTENTS

CHAPTER I INTRODUCTION

CHAPTE II CARBONIZATION AND GRAPHITIZATION

CHAPTER III OPTICAL CRYSTALLOGRAPHY OF MESOPHASE

CHAPTER IV EXPERIMENTAL DETAILS

CHAPTER V EXPERIMENTAL RESULTS AND DISCUSSION

CHAPTER VI CONCLUSIONS

CHAPTER I   INTRODUCTION

1.1 Introduction

1.1 INTRODUCTION

The synthetic manufacture of graphite has become more interesting and got recognition in the new material science of organic materials since 1961 after the discovery of mesophase transformation by Brooks and Taylor [1-4]. The expansion of this interest is continued, as carbon exhibits potential applications in new areas.

The pyrolysis of organic compounds in the temperatures between 350^0C -600^0C is the most important process for the production of carbons [5-8]. This new approach to graphite fabrication have been developed from the study of carbonaceous mesophase.

The mesophase transformation takes place in organic materials starting from single benzene ring to higher aromatic rings during pyrolysis at the temperatures between 350^0C and 600^0C. During the heat-treatment of polycondensed aromatic hydrocarbon, thermal decomposition and thermal polymerization reactions takes place.

For graphitizing carbons, the size of the elemental domains of the bulk mesophase is evaluated by measuring the isochromatic areas of course mosaics in the optical micrographs. The smallest domains correspond to non-graphitizing carbons. The ability to graphitize of any carbonaceous material is thus predetermined entirely by the size of the elemental domains of the bulk mesophase.

The graphitizing carbons are generally formed from substances containing more hydrogen, and less oxygen. Substances including the vitrinites of medium volatile coking coal, high temperature coal tar pitch, petroleum bitumens, polymers such as

polyvinyl chloride and poly-nuclear aromatic compounds such as napthacene and dibenzenthrone belong to the group of graphitizing carbon. This substances pass through a plastic stage on heat-treatment [9-11]. The crystallites remain relatively mobile during the early stages of carbonization and cross linking in the mass is weak. The structure is more compact and there is in all stages a strong tendency for neighbouring crystallites to arrange themselves nearly parallel to one another, leaving only small holes between the basal planes of neighbouring groups.

Formation of the anisotropic mesophase is a function of heat-treatment temperature and duration of heat-treatment [12-14]. As carbonization progresses with increasing temperature and duration of heat-treatment, the growing mesophase spherules, which are more dense than the isotropic parent phase, sink to the bottom of the container. When spherules meet coalescence occurs to produce larger droplates, leading eventually to a bulk mesophase. When viewed microscopically with cross polarizers, the bulk mesophase displays a complex ensemble of extinction contours. The polarized-light extinction contours display nodes and crosses. The processes of the formation, coalescence and deformation of the plastic mesophase establishes the basic elements of the graphite microstructure.

Reflected polarized-light microscopy using crossed polarizers with a gypsum plate has been employed to investigate the microstructure of carbonaceous mesophase formed at the early stage of carbonization. It follows from the changes in pleochroism and isogyres occuring with the stage rotation, that a simple mesophase spharule is optically a uniaxial positive liquid crystal belonging to the hexagonal system with a straight extinction i.e., the parallel alignment of the aromatic layer planes and the rearrangement of the hexagonal ring structure viz. the graphite structure.

The technique of differential thermal analysis (DTA) has been employed as an additional information to study the structural changes occuring in the organic materials under heat-treatment [15]. These changes may be due to dehydration, transition from one crystalline variety to another, destruction of crystalline lattices, oxidation, decomposition etc.. This technique has recently attained considerable importance in determining the carbonizing and graphitizing properties of pure organic compounds, coals and pitches, etc. .

Some more additional informations are also necessary to supplement the polarized-light and DTA techniques to interpret the above result still more correctly. These are thermogravimetric analysis (TGA), X-ray diffraction, infrared absorption spectroscopy, etc..

Thermogravimetric analysis (TGA) involves the determination of weight loss from a sample as a function of time or temperature [m=f(t or T)] while a sample is heated or cooled at a constant rate. This technique is effective for quantitative analysis of thermal reactions that are accompanied by mass changes due to release of volatile matter, evaporation, decomposition, gas absorption, desorption and dehydration.

In the graphitic carbon, the extent of ordering that is associated with increaseing order of graphitization can be estimated from X-ray diffraction pattern. With increasing carbonization, the interplanar spacing of carbon hexagonal planes decreases and approaches a regular crystalline structure to that of graphite [16-17].

Infrared spectroscopic study provides valuable information concerning the nature and variation with carbon content of the substituent groups as well as the nature of

3

the aromatic systems [18-19]. Under heat-treatment the existing functional groups have been identified by the IR spectroscopic study.

The objective of this research is to see whether the degree of graphitization increases with increasing of number of rings in the aromatic compounds and to have a better understanding of the optical properties of anisotropic carbons.

The order of the degree of graphitization can be ascertatined from the following studies: (i) the change in the interlayer spacing by X-ray diffraction study; (ii) the broadening of the peak area of the aromatic band region by IR study; (iii) the mesophase transition study by a combination of DTA analysis and polarized-light technique. The optical anisotropic observation will be carried out by polarized light microscopy.

REFERENCES

1.1   Taylor, G. H., Fuel 40, 465, 1961.

1.2   Brooks, J. D. and Taylor, G. H., Nature, 206, 697, 1965.

1.3   Brooks, J. D. and Taylor, G. H., Carbon, 3, 185, 1965.

1.4   Brooks, J. D. and Taylor, G. H., Advan. Chem. Ser. 55, 549, 1966.

1.5   Brooks, J. D. and Taylor, G. H., "Chem. and Phy. of Carbon" (Walker, P. L. Jr., Ed.), Marcel Dekker, New York, 4, 243, 1968.

1.6   Hossain, T. and Dollimore, J., Thermochimica Acta, 108, 211, 1986.

1.7   Podder, J. and Hossain, T., Thermochimica Acta, 137, 225, 1989.

1.8   White, J. L., Guthrie, G. L. and Gardner, O., Carbon, 5, 517, 1967.

1.9   Kipling, J. J., and Shooter, P. V., Carbon 4, 1, 1966.

1.10   Honda, H., Kimura, H., Sanada, Y., Sugawara, S. and Furuta, T., Carbon, 8, 181, 1970.

1.11   Dubois, J., Agace, C. and White, J. L., Euratom Report 4627e, 1971.

1.12   Honda, H., Kimura, H. and Sanada, Y., Carbon, 9, 695, 1971.

1.13   Sanada, Y., Furuta, T., Kimura, H. and Honda, H., Fuel, 52, 143, 1973.

1.14   White, J. L., In petroleum-Derived Carbons (Edited by Gardy, T. M. O. and Deviney, M. I.), Am. Chem. Soc. Symp. Ser., 21, 282, 1976.

1.15   Rashid, M. A., Hossain, T. and Asgar, M. A., Thermochimica Acta, 259, 263-268, 1995.

1.16 Kinney, C. R., Nunn, R. C. and Walker, P. L., Industrial and Engineering Chemistry, 49, 880, 1957.

1.17 Mentser, M. et al., Proc. 5th Carbon Conf., Pergamon Press, 2, 493, 1962.

1.18 Robeot, T. C., Infrared Spectroscopy, 2nd Edition, 1975.

1.19 Silverstein, R. M., Bassler, G. C. and Morril, T. C., Spectrometric Identification of organic Compounds, John Willey & Sons., NY, 1981.

CHAPTER II CARBONIZATION AND GRAPHITIZATION

2.1 INTRODUCTION

Carbon is the sixth element in the periodic table and it has atomic weight 12.011 on the chemical scale. The electron configuration in carbon is $1s^2 2s^2 2p^2$. Of the six electrons in a neutral atom, four in the outer L-shell, $2s^2 2p^2$, are the ones available for chemical bonding, principally by the excitation of one S-electron into a P-state, followed by orbital mixing. Several hundred thousand compounds containing the element carbon are known till today, because of this unique atomic structure of carbon which results in its ability to react chemically with most other elements.

During the heat-treatment of carbon containing materials to high temperatures, the removal of non-carbon atoms, usually oxygen, hydrogen, nitrogen or sulphur, as well as some carbon constitutes, the process what is known as 'carbonization'. This process follows a rearrangement of order within the remaining carbon atoms giving a greater degree of order within the carbon produced which may develop a three-dimensional order. Simply this development of a three-dimensional order which produces a structure very close to the well-defined structure of pure graphite is termed 'graphitization'. In fact, graphitization does not occur in 'graphitizable carbons' until they are annealed above 2500^0C. The temperature range from 2500^0C to 3000^0C is called the 'graphitization temperature range'.The temperature of the onset of graphitization has been found to vary and is dependent on the parent material.

2.2 DIFFERENT FORMS OF CARBON AND CRYSTALLOGRAPHIC MODELS

There are only two allotropic crystalline forms of carbon i.e., graphite and diamond. Both occur in nature or can be produced artificially from many carbon

containing materials. The difference in properties between these two allotropic forms is determined by the forces lying within and between crystallites. Diamond is a face-centred cubic material with each carbon atom bonded covalently to four others in the form of a tetrahedron, the interatomic distance being 1.54A. It is the hardest naturally occurring substance due to the rigidness of the tetrahedral covalent bond lattice of the single macromolecule that forms the perfect crystal. Diamond is metastable to graphite, the conversion of graphite into diamond requiring the assistance of catalysts and high temperatures and pressures. Though diamond normally has the structure described above, Ergun and Leroy [1] have shown that a hexagonal structure for diamond is possible. Again diamond changes spontaneously to graphite at ordinary pressure above 1500^0C [2]. Thermodynamically, graphite at atmospheric pressure is the more stable form of carbon.

Graphite is a laminar structure and is the anisotropic allotropic form of carbon. Its accepted ideal crystal structure is illustrated in Fig. 2.1, which was first established by Bernal [3]. It is a stable hexagonal lattice where the basal planes or layer planes consist of open hexagons with interatomic C-C distance $1.415A^0$. These planes are arranged in an alternating sequence, the interplaner distance being 3.354A. Crystallographically perfect graphite has a density of 2.266g/ml. In this structure only three of the four valence electrons of carbon form regular covalent bonds with adjacent carbon atoms. The free fourth electron resonates between the valence bond structure s. Strong chemical bonding forces exist in the basal planes whereas weak Vander Walls' forces exist between planes. The bonding energy between planes is only about 2% of that within the planes [4,5]. The weak forces between layer planes account for (a) the tendency of graphite materials to fracture along planes, (b) the formation of interstitial compounds, and (c) the lubricating, compressive

and many other properties of graphite. As shown for the hexagonal graphite structure, the stacking sequence of the planes is ABAB so that the atoms in alternate planes are congruent.

A rhombohedral structure has been found to exist in many graphites where the stacking sequence is ABC ABC (Fig. 2.2). Lipson and Stokes [6] were able to show that this rhombohedral lattice, originally proposed by Debye and Scherrer [7] fully accounted for the X-ray lines found in some powder photographs of graphites. The proportion of the rhombohedral form may be increased in graphites by grinding [8] which indicates that the change arises from the movements of the layers of carbon networks with respect to one another.

Most naturally occurring graphite is polycrystalline. Perfect single crystals greater than 10μm are quite rare, although they can be produced with difficulty. Most synthetic graphites, made by high temperature calcination of pitch/coke blends, are polycrystalline. Single crystals of graphite occurring in some natural deposits of graphite near perfect single crystals of quit large dimensions can be obtained by pyrolytic deposition of carbon from carbonaceous vapurs. Under suitable conditions, the deposit of carbon can take the form of highly oriented layers. Subsequent treatment of this material can produce quite large single crystals of pure graphite. Such graphite is known as 'pyrolytic graphite'.

A third form of carbon, apart from diamond and graphite, exists which is known as 'amorphous carbon'. Although this name literally means a structureless form of carbon, almost all amorphous carbon possess a small amount of order. The first application of X-ray diffraction methods to amorphous carbons, however, led to the concept that they were also graphitic with their apparently amorphous character

which arises from the very minute size of the crystallites. These amorphous carbons can be prepared by the combustion of hydrocarbons in an incomplete supply of air, i.e., carbon blacks, and include soot, charcoal, and lamp blacks.

2.3 STRUCTURE OF CARBONS AS REVEALED BY X-RAYS

Carbons can be classed into two distinct and well-defined types: graphitizing or non-graphitizing, soft or hard. Graphitizing carbons are generally relatively soft, are of high apparent density, possess little microporosity and are relatively rich in hydrogen or low in oxygen, sulpher and nitrogen. They were termed 'soft carbons' by Mrozowski [9]. Franklin considered that, during the early stages of the carbonization process, the crystallites in the graphitizing carbons were fairly mobile and that in the region of $1000^{0}C$, a high proportion of the crystallites lay nearly parallel to each other. Weak cross-linking was thought to exist between the crystallites. A model (reproduced in Fig. 2.3) was put forward by Franklin [10] for the structure of a graphitizing carbon. X-ray data suggested that the whole layers or groups of layers moved on increasing the heat-treatment temperature but the most significant factor was that neighboring crystallites had to be nearly parallel. Crystallite growth was considered to occur by the layer planes linking togather.

Non-graphitizing carbons are generally hard, are of low apparent density, have high microporosity and are relatively low in hydrogen or rich in oxygen, sulphur and nitrogen. They were correspondingly called 'hard carbons' by Mrozowski [9]. Again Franklin [10] put forward a model (reproduced in Fig. 2.4) to account for their structure. In this model he considered that the parallel layer groups which were oriented at all angles, were joined together at their extremities, thus accounting for the microporosity. With the increase of heat-treatment temperatures

there was some growth in the basal plane direction by incorporation of disordered carbon atoms at the edges of the crystallites. Other carbon atoms acted as linkages between crystallites.

2.4 CRYSTALLOGRAPHIC PARAMETERS

Graphitization can be observed by certain changes in some measurable crystallographic parameters. The main parameters are:

(a) The d-spacing which decreases from the turbostratic value of 3.44A towards the graphitic value of 3.354A.

(b) The apparent layer diameter, L_a, which increases on graphitization.

(c) The apparent layer plane height, L_c, or alternatively, the number of layers, M, in a parallel layer packet, which also increase on graphitization.

(i) Maire and Mering's g-factor

This graphitization factor proposed by Maire and Mering [11,12,13] is a purely empirical quantity indicating the position of the material on a scale of which the two fixed points are the turbostratic and graphitic spacings and is simply defined from the apparent layer spacings a_3 (in A) as

$$a_3 = 3.354 \, g + 3.440 \, (1\text{-}g) \qquad \text{------------------- 2.1}$$

It increases with increasing heat-treatment temperature for graphitizing carbon.

(ii) The Franklin/ Bacon-Parameter

The p-parameter was first postulated by Franklin [10] as the probability that a random disorientation occurs between any two neighboring layers. Its value varies

from unity for a turbostratic graphite-like structure (where the hexagon layers are parallel to each other but not stacked in any crystallographic order) to zero for a perfectly graphitic structure. This led to the following parabolic relationship between p and d, the interlayer spacing:

$$d = 3.440 - .0.086 (1 - P^2)$$ ------------------------- 2.2

d- spacing again being expressed in A.

The above equation was slightly modified by Bacon [14,15] to account for the fact that the influence of an oriented packet will extend beyond the layers immediately adjacent to it. The modified equation was given as

$$d = 3.440 - 0.0866 (1-P) - 0.064P (1-P) - 0.030 P^2 (1-P)$$ ------------------ 2.3

where the d - spacings again were in A.

This modified relationship gave better arrangement with experimental data than equation (2.2). For a graphitizing carbon the apparent value of d decreases with the rise of heat-treatment temperature and p falls from near unity to near zero.

(iii) Warren's P_1-Factor

Warren [16] in a study of carbon blacks defined P_1 as the probability that two adjacent layers should be correctly oriented. P_1 can be obtained from the following linear relation

$$d = 3.35 + 0.09 (1-P_1)$$ ------------------- 2.4

where the value of d is again expressed in A.

2.5 CARBONIZATION PROCESS

It has been pointed out by many workers that the early stages of carbonization (350-600°C) are important in determining the ability to graphitize at high temperature. The following is a brief review of the work done.

Kipling et al. [17] described some of the properties of carbons made from a range of polymers and one polycyclic compound (dibenzanthrone). The carbons could be sharply divided into two groups; those which became graphitic at temperatures of 2700°C or above and those which remained non-graphitic. Kipling has investigated the relationship between fusing during carbonization process and the ability of the resultant carbon to graphitize at a higher temperature. It was later suggested [18,19] that materials of the kind examined could only give rise to graphitic carbon if they passed through a fusion stage which had to occur under specific conditions. These specific conditions were such that the polycyclic aromatic structures formed in the residue during carbonization readily orientated to form graphite. It was confirmed by using polarized-light microscopy to study low and high temperature carbons [20]. Taylor [21] carried out a detailed study of the microscopic changes exhibited by a vitrinite with progressive carbonization using optical methods. Observations were made with samples of a thermally metamorphosed coal. The vitrinite, which in its unaltered state was anisotropic, became isotropic and this transition was followed under controlled conditions in the laboratory. The change from anisotropy to isotropy was observed to occur at a temperature slightly below that at which the plasticity became measurable. About 10°C to 15°C before the onset of resolidification the change from isotropic plastic vitrinite to anisotropic semicoke was indicated by the appearance of small spherules initially of micron size, in the isotropic vitrinite, forming as a separate

phase. These spheres were observed to grow in size with the increase in heat-treatment temperature at the expense of the plastic vitrinite which eventually formed, by coalescence, a mosaic structure about the resolidification temperature.

The spheres, which later became units of the mosaic texture, had an interesting pattern of behavior in singly and doubly polarized light. A particular structure having a strain effect was put forward to account for this behavior. At first it was thought that this structure was inherently improbable as because the strain effects were in fact of little importance to account for the observed optical properties, and so a second model which included a stress effect was proposed. However the original structure was later verified to be correct by Brooks and Taylor [22,23] using electron diffraction and optical microscopic techniques. The structure of a simple sphere has been shown in Fig. 2.5 & 2.6 in three dimensions. The layers consist of condensed polycylic aromatic compounds which are aligned perpendicular to the polar diameter but curve to meet the interface with the isotropic matrix at a high angle. The poles constitute anomalous regions, but this is reflected in little if any departure of the droplet from sphericity. Brooks and Taylor also showed that sphere growth also occurred on heating bitumen, pitches, polyvinyl chloride (PVC), naphthacene and dibenzanthrone, all of which produce graphitizing carbons. This two phase liquid state structural transformation is known as 'carbonaceous mesophase formation' or 'liquid crystal formation'.

Brooks and Taylor concluded that those materials which ultimately produce graphitizing carbons, generally pass through a fluid stage during carbonization in the temperature range 350°C-600°C. In the final stages of this fluid phase a second phase possessing anisotropic structures forms and that this structure persists into the semi coke beyond. They also concluded that any solid surface appeared to be a

preferred site for mesophase growth and that the nucleating effect of solids increased with their available surface area. It is now thought, however, that nucleation is not the principal mechanism in mesophase formation but that the growth of the anisotropic liquid crystals occurs at the expense of the isotropic liquid phase [24].

White et al. [25] used polarized-light micrography to investigate the microstructure of the coalesced mesophase formed in the carbonization of coal-tar pitch. They noticed that the structural features of the coalesced mesophase were similar to those found in electron micrographs of graphitized materials. Also prominent features in the polarized light extinction contours were the nodes and crosses which did not move when the plane of polarization of the incident light was rotated. These nodal points were found to correspond to two types of linear defects in the stacking of the aromatic layer planes.

Later white and co-workers [26] extended their classification of defect structures in the stacking of the mesophase layer planes to four. They are : (a) co-rotating node (b) counter-rotating node (c) co-rotating cross (d) counter-rotating cross (Fig .2.7]. These four classes of linear defects were termed as above depending on whether the extinction contours moved with or against the direction of rotation of the plane of polarization of the incident light. The notation used there is an opposition to that used by Honda et al. [28].

White et al. concluded that the processes of the formations, coalescence and deformation of the plastic mesophase established the basic elements of the graphite microstructure, i.e., the parallel alignment of the aromatic layer planes and the rearrangement of the complex folds in the fibrous regions. The linear stacking

discontinuities, namely the nodal and cross structures, were essential features of the coalesced mesophase, and the nodal structures at least were found to persist in their basic form upto graphitization temperature. However, they did not seem to be involved in shrinkage cracking, fold sharpening and the formation of mosaic block and kinks which occurred during heat-treatment. Later white et al. [27] extended their studies to include graphitizable materials such as coal-tar pitch and petroleum coke feedstocks and arrived at similar conclusions.

Honda and co-workers [28] supplemented the works of Brooks and Taylor by examining in much more detail, the effect of temperature and soaking time upon the growth and physical properties of the mesophase in pitches and found that the temperature and duration of heat-treatment were essentially complementary factors. In a polarized-light study Honda et al. [29] employed crossed polarizers with a gypsum plate to investigate the microstructure of the carbonaceous mesophase formed in the early stages of carbonization of pitches. By use of this so-called sensitive-tint technique, changes in pleochroism and in extinction contours for coalesced and for deformed mesophase were observed.

Honda also explained schematically how the crosses and nodal structures were formed by the coalescence of two simple spherules and the deformation of such coalesced mesophase.

Whiltaker and Grindstaff [30] found that the rates of formation, growth and coalescence of the mesophase spheres varied from feedstock to feedstock and that the type of molecular structure in the original feedstocks and the type of structures formed on heat-treatment had a significant influence on the resulting coke structure.

2.6 PRESSURE EFFECTS ON MESOPHASE MICROSTRUCTURE

Extensive studies on the carbonization of some organic compounds and coal-tar pitches under extremely high pressures (~3K bar) were performed by Walker et al. [31,32] and by Marsh et al. [33,34]. The structures of the solid products carbonized in a sealed tube surrounded by a hydrothermal pressure bomb, were characterized as anisotropic carbonaceous mesophase, whose morphologies changed from vesicular to spherical with increasing pressure. Pressure was also observed to hinder or to prevent coalescence of the mesophase and to enhance graphitizability.

Some results on studies with conventional coal-tar and petroleum pitches [36,37] under pressure upto 200 bar showed that increasing pressure does not only increase the coke yield but also lowers the temperature at which pyrolysis is completed. It was also shown that increasing pressure improves preorder and graphitizability of the residues. Increasing pressure causes a pronounced segregation of original insolubles of conventional coal-tar pitches and of artificial insoluble like carbon black. The separated insolubles accumulate in the upper part of the pyrolysis vessel whereas a highly ordered mesophase without insoluble is found lower down.

2.7 DIFFERENT TYPES OF MESOPHASE SPHERULES

Since the first report of carbonaceous mesophase spherules of optical anisotropy by Brooks and Taylor [22,23] a large number of studies were made on the related subject, e.g., the nucleation, growth and coalescence processes of mesophase spherules [38-40]. Most of the studies confirmed the findings of Brooks and Taylor that in the individual mesophase spherule flat aromatic molecules lie

parallel to each other in the interior and perpendicular to the surface of the spherule near the surface.

Most recently mesophase spherules with structure other than that proposed by Brooks and Taylor have been reported. Honda and his co-workers [41] reported a second-type mesophase spherules with different optical properties from those of the Brooks-Taylor spherules and proposed a structural model having the outer layers lying parallel to the spherule surface but a similar layer alignment to the Brooks-Taylor type spherules around the central region of the spherule (Fig. 2.8b). Similar mesophase spherules were also found by Kovac and Lewis [42] and Imamura et al. [43]. Hüttinger [44] and also Imamura and Nakamizo [45] reported the third-type mesophase spherules with all the layers lying in concentric circles about the centre of the spherules (Fig. 2.8c). The structure of a fourth-type spherule (Fig. 2.8d) was reported by Imamura, Nakamizo and Honda [46]. The structure of this type was very similar to that of the Brooks-Taylor type and it is now believed that the fourth-type spherule is a metastable phase of the Brooks-Taylor type. Novel anisotropic mesophase features having a flower-petaloid texture were reported by Mochida et al. [47].

2.8 THERMAL BEHAVIOR OF GRAPHITIZING CARBONS

Carbonaceous materials such as kerogen, coals, heavy petroleum products, higher aromatics etc. of various origin whether pyrolyzed or coalified, follow the same microstructure trend of graphitizing carbons. On carbonization, the graphitizing carbons soften first and possess a visco-elastic stage and gradually falls down to a minimum viscosity [48] and then coalesce and finally increases again up to the brittle solid state which is known as the semi-coke stage. Fig. 2.9 shows the thermal

behavior of graphitizing carbon. At higher temperatures as the material progressively graphitizes, an increasing number of layer pairs align in the AB sequence and reach the 3.354A interlayer spacing of graphite.

All the carbonaceous materials follow the same graphitization process, whatever the degree of crumpling of their layers. Before the semi-coke stage bulk mesophase made of individual BSU's are formed. Then distorted and wrinkled layers appear below 2000^0C . When heat-treatment temperature (HTT) increases further, flat lamellae give flat polycrystalline graphite whereas curved pores give polyhedral pores more or less graphitized. The smaller the elemental domains of the initial bulk mesophase (pore wall's), the smaller the polyhedral pores and the smaller the final degree of graphitization reached at 2900^0C and the smallest domain correspond to non-graphitizing carbons. The ability to graphitize any carbonaceous material is thus predetermined entirely by the size of the elemental domains of the bulk mesophase, i.e., the total molecular orientation (MO).

2.9 LOW TEMPERATURE CARBONIZATION

Carbonization is a complex process in which polymerization plays a dominant role during which the original organic matter undergoes loss of its non-carbon elements usually oxygen, hydrogen, nitrogen or sulphur, as well as some carbon as the temperature rises. These elements are evolved as gases, usually in combination with part of the carbon, and this process follows a rearrangement of order within the remaining carbon atoms which may develop a greater degree of three-dimensional order.

Three overlapping phases are usually identified in the carbonization process. The boundaries between the phases are defined by temperature levels whose absolute values vary with the character of the material undergoing carbonization.

In the first phase of 'precarbonization' possibly (between 150^0C and 400^0C), some bond-breaking reactions and reduction of hydrogen bonding occur, which may lead eventually to melting. Some light species, which exist as guest molecules or are formed by the breaking of very weak bonds, are released. Some important molecular rearrangements, condensation reactions and 'molecular stripping' also take place, and there is little change in the optical properties of the majority of organic materials.

During the second phase, the softening or the formation of liquid from the organic matter transforms into an optically anisotropic mesophase, a three-dimensional bonding early in aromatic condensation. If, the aromatic condensation takes place, then the carbon produced will have much greater ordering due to the development of progressive alignment of aromatic layers or lamellae in groups which form 'crystallites'.

In the third phase of carbonization (650^0C to 1500^0C), after resolidification, reactions take place principally in the solid state. The carbonaceous product may evolve secondary gases, mainly Co and H_2, while undergoing condensation.
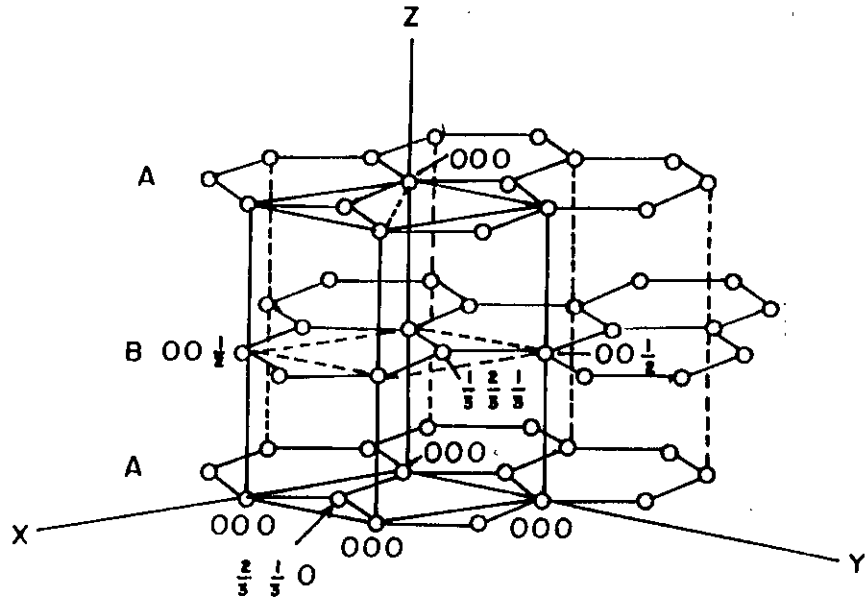
Fig 2.1   The ideal graphite crystal structure with the hexagonal unit cell with crystal axes and lattice co-ordinates.
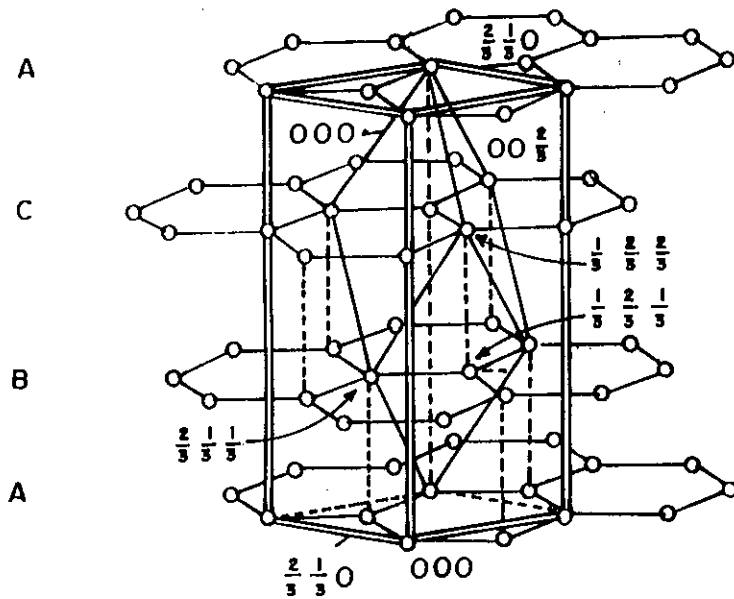
Fig 2.2   The rhombohedral structure, showing the true unit cell and the atomic co-ordinates in the approximate hexagonal cell shown in double lines.
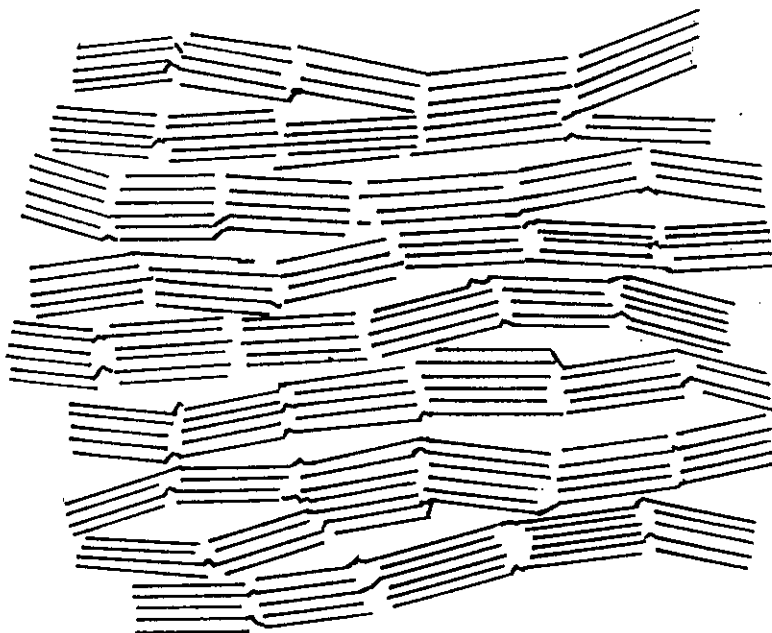
Fig 2.3   Schematic representation of the structure of a graphitizing carbon.
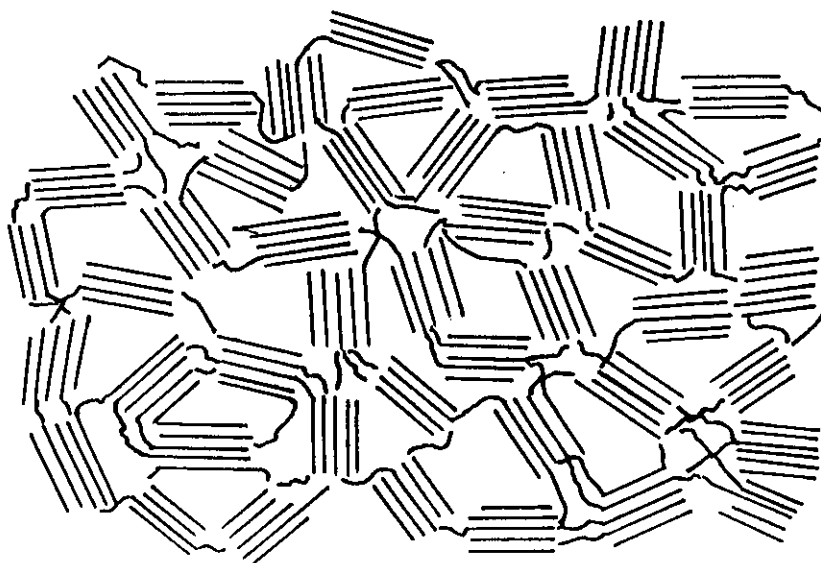
Fig 2.4   Schematic representation of the structure of a non-graphitizing carbon.

POLE

POLE
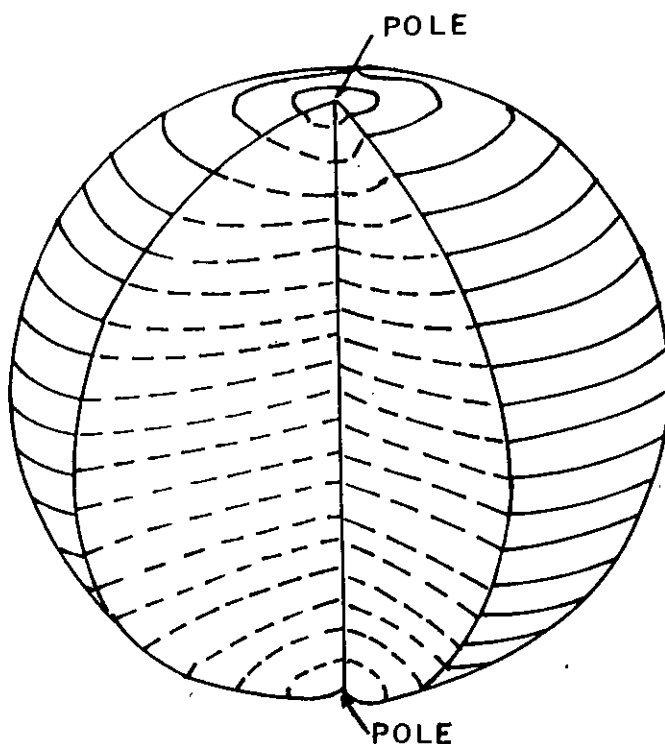
Fig 2.5   Mesophase sphere with section including polar diameter

BEFORE   CONTACT

JUST   AFTER   CONTACT

SHORT   TIME   AFTER   CONTACT

TYPE OF COMPLEX INTERNAL STRUCTURE FORMED
WHEN COMPOSITE OF TWO OR MORE SPHERES
CONTRACTS TO ONE LARGE SPHERE
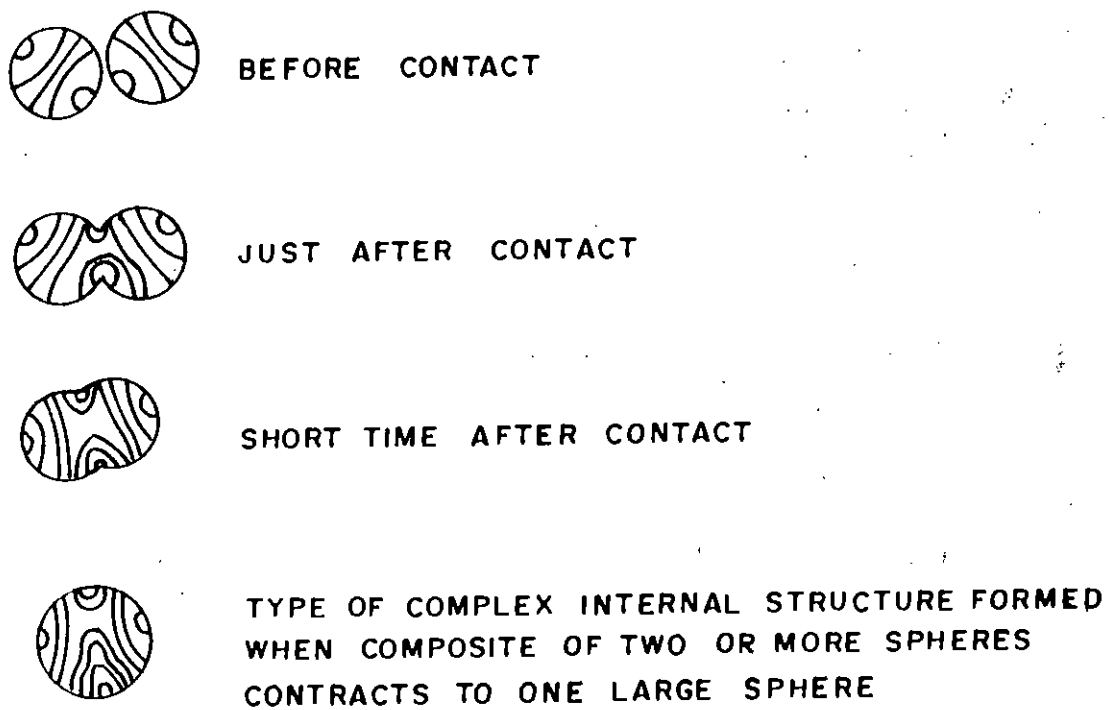
Fig 2.6   Rearrangements which appear to occur when two spheres coalesce

CO - ROTATING
CROSS

COUNTER ROTATING
NODE

CO-ROTATING
NODE

COUNTER ROTATING CROSS

PLANE OF POLARIZATION
OF INCIDENT LIGHT

DIRECTION OF ROTATION
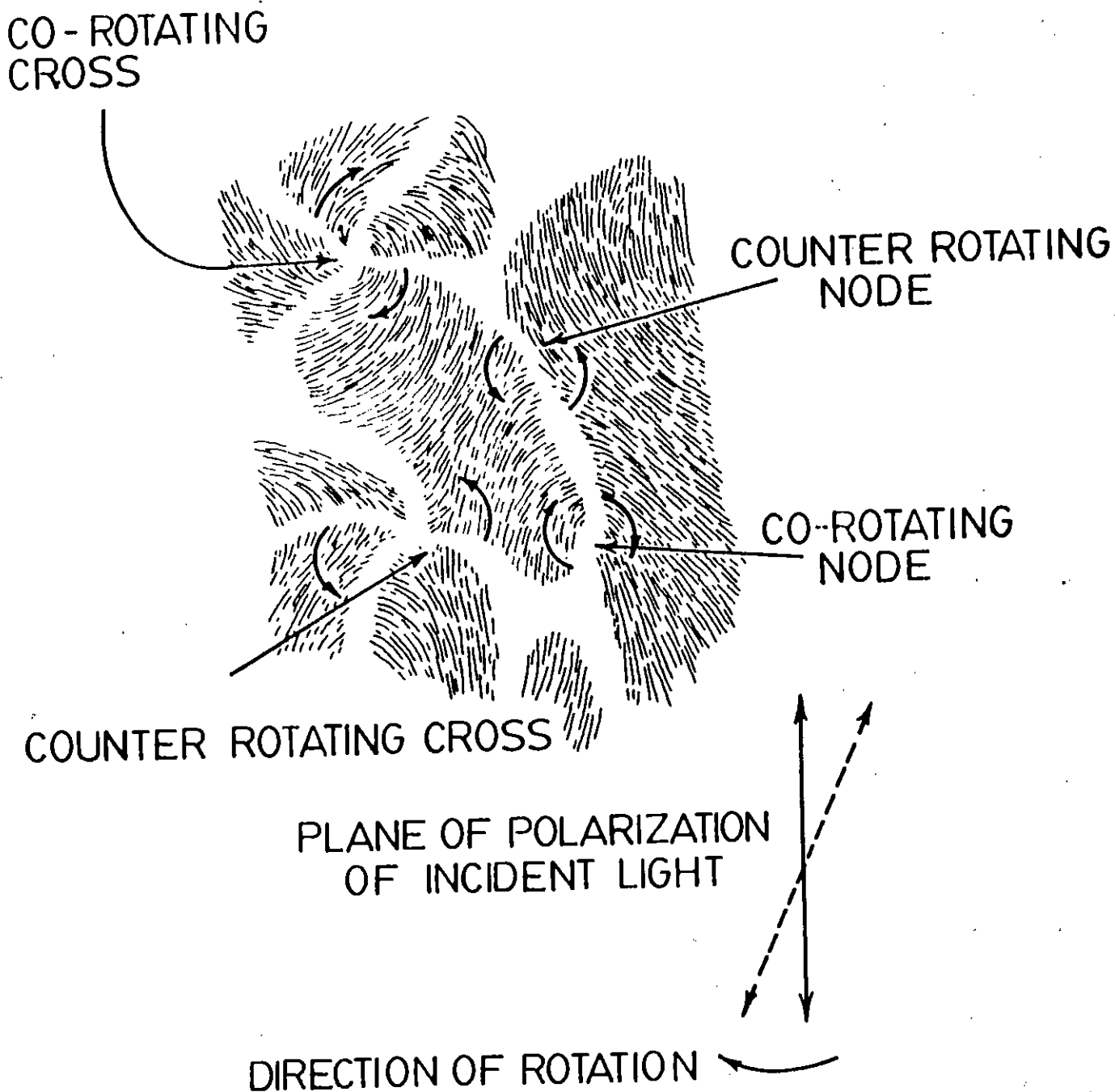
Fig 2.7   Schematic diagram of the four types of mesophase stacking defects.
Extinction contours are shown for the case of crossed polarizers.

	BROOKS-TAYLOR TYPE	2ND TYPE	3RD TYPE	4TH TYPE
SECTION				
MODEL				
	(A)	(B)	(C)	(D)
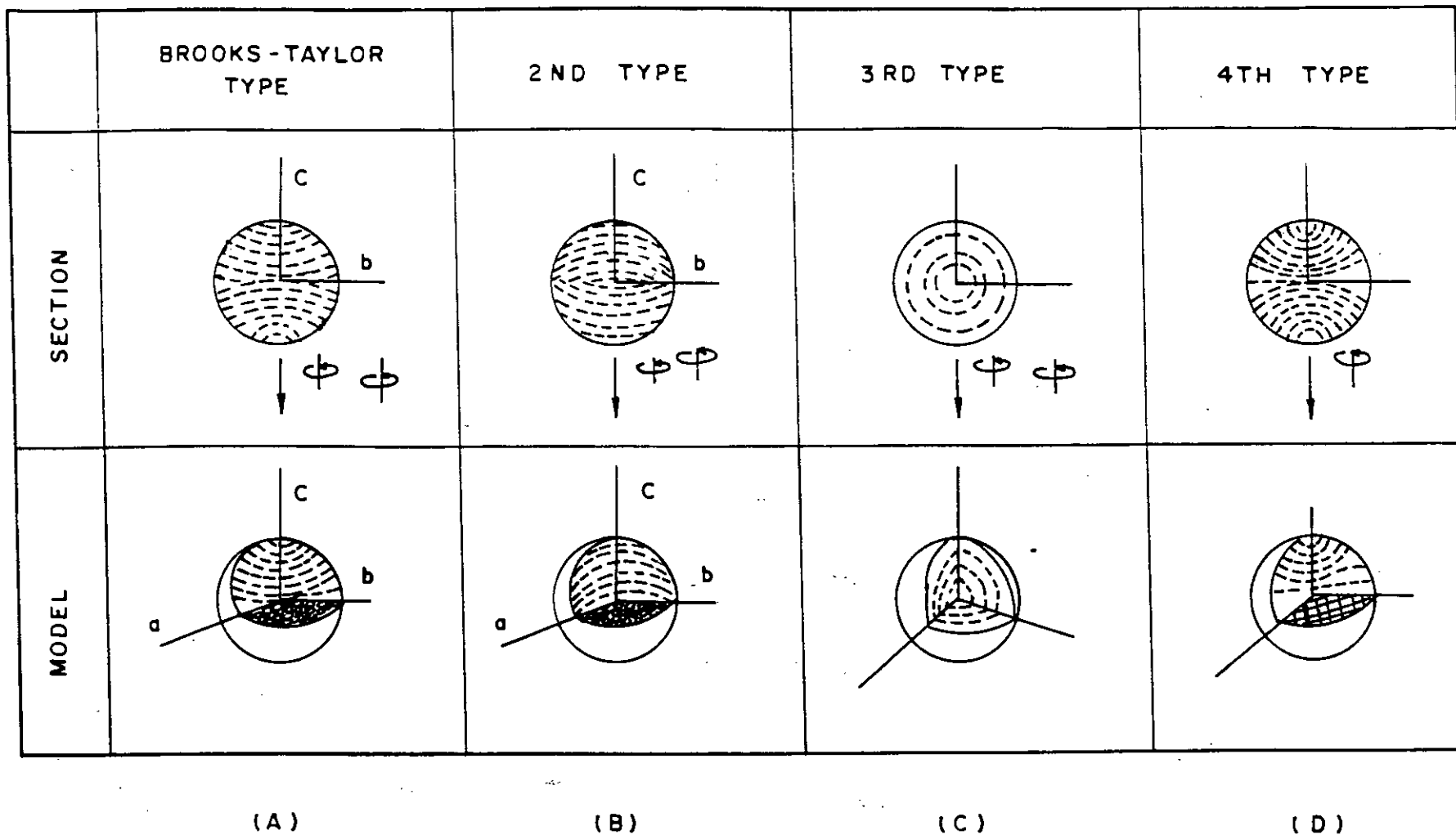
Fig 2.8 Schematic structural sketches of sections and three-dimensional models for (A) Brooks-Taylor type, (B) 2nd type, (C) 3rd type, and (D) 4th type spherules.
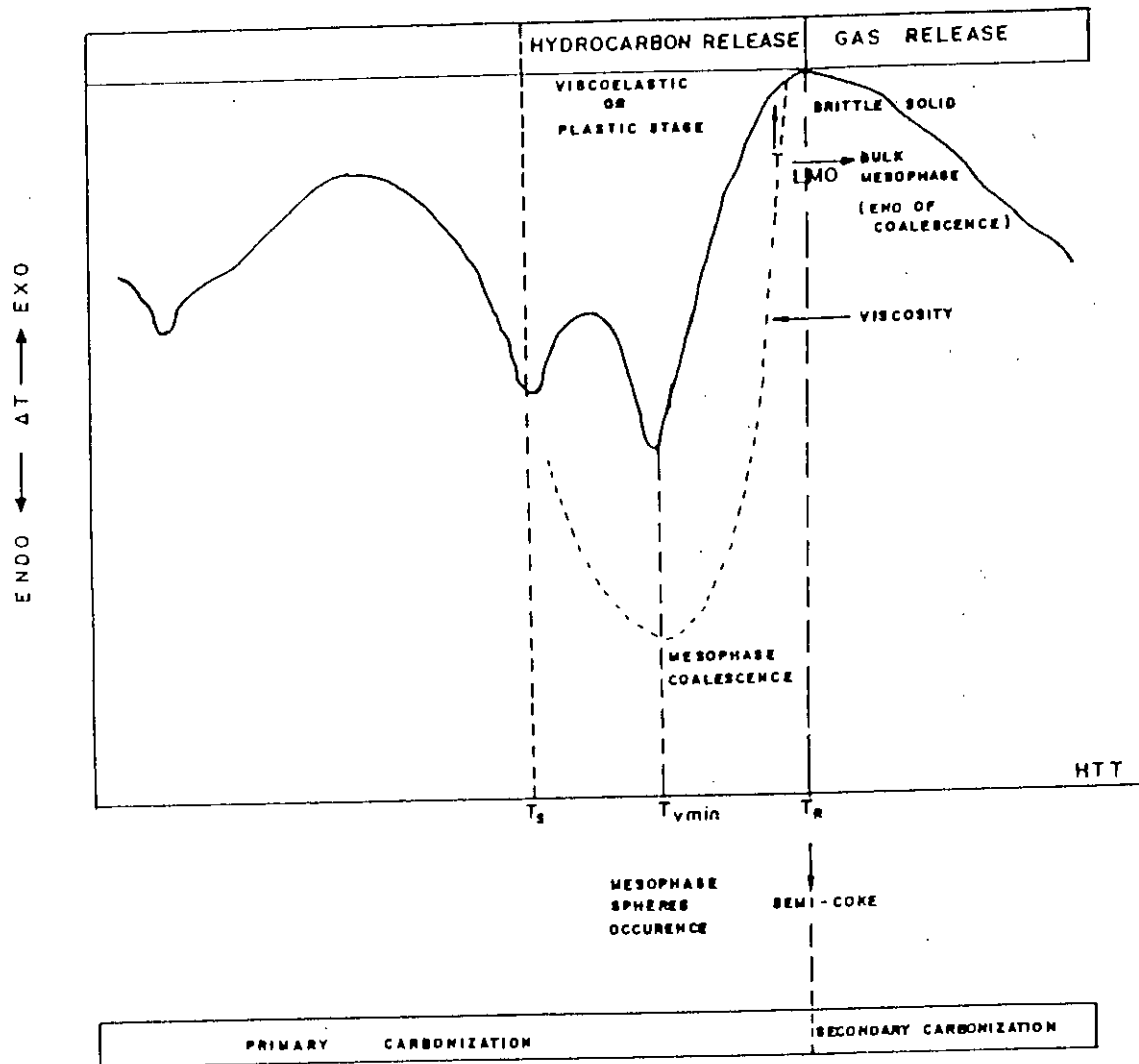
Fig. 2.9   Schematic sketch of the carbonization of a graphitizing carbon. Where T_s, softening temperature. T_{vmin}, the temperature of the minimum viscosity (mesophase nucleation), T_R the resolidification temperature, T_{LMO} the temperature of bulk mesophase formation (end of coalescence and hardening). The Solid line corresponds to the DTA, the dashed line corresponds to the viscosity.

REFERENCES

2.1   Ergun, S., Leroy, E. A., Nature, 195, 765, 1962.

2.2   Seal, M., Nature, 185, 522, 1960.

2.3   Bernal, J. D., Proc. Roy. Soc. A., 106, 749, 1924.

2.4   Girifalco, L. A. and Lad, R. A., J. Chem. Phys., 25, 693, 1956.

2.5   Brennan, R. O., J. Chem., Phys., 20, 40, 1952.

2.6   Lipson, H. and Stokes, A. R., Proc. Roy. Soc. A, 181, 101, 1942.

2.7   Debye, P. and Scherrer, P., Physikal, Z., 8, 291, 1917.

2.8   Bacon, G. E., Acta Cryst., 3, 320, 1950.

2.9   Mrozowski, S., Proc. First and Second Conf. on Carbon, Buffalo, 31, 1953.

2.10   Franklin, R. E., Proc. Roy. Soc. A, 209,196, 1951.

2.11   Maire, J. and Mering, J., First Conf. Ind. Carbon and Graphite, Soc. Chem. Ind., 204, 1957.

2.12   Maire, J. and Mering, J., Proc. Third Carbon Conf., Buffallo, 337, 1957.

2.13   Maire, J. and Mering, J., Proc. Fourth Carbon Conf., Buffallo, 345, 1957.

2.14   Bacon, G. E., Acta Cryst., 4, 558, 1951.

2.15   Bacon, G. E., U. K. A. E. A. Report AEREM/R2702, 1958.

2.16   Warren, B. E., Proc. Second Carbon Conf., Buffalo, 49, 1955.

2.17   Kipling, J. J., Sherwood, J. N., Shooter, P. V. and Thompson, N. R., Carbon, 1, 315, 1964.

2.18   Kipling, J. J., Sherwood, J. N., Shooter, P. V. and Thompson, N. R., Carbon, 1, 315, 1964.

2.19   Kipling, J. J., and Shooter, P. V., Second Conf. Ind. Carbon and Graphite, Soc. Chem. Ind., 15, 1965.

2.20   Kipling, J. J., and Shooter, P. V., Carbon, 4, 1, 1966.

2.21   Taylor, G. H., Fuel, 40, 465, 1961.

2.22   Brooks, J. D. and Taylor, G. H., Nature, 206, 697, 1965.

2.23   Brooks, J. D. and Taylor, G. H., Carbon, 3, 185, 1965; Physics & Chemistry of Carbon, 4, 243.

2.24   Walker, P. L., Carbon, 10, 369, 1972.

2.25   White, J. L., Guthrie, G. L. and Gardner, J. O., Carbon, 5, 517, 1967.

2.26   White, J. L., Dubois, J. and Souillart, C., J. Chim. Phys., Special Volume, April, 1969, 33; Euratom Report 4094e, 1969.

2.27   Dubois, J., Agace, C. and White, J. L., Euratom Report 4627e, 1971; J. Metalography, 3, 337, 1970.

2.28   Honda, H., Kimura, H., Sanada, Y., Sugawara, S. and Furuta, T., Carbon, 8, 181, 1970.

2.29   Honda, H. Kimura, H. and Sanada, Y., Carbon, 9, 695, 1971.

2.30   Whittaker, M. P. and Grindstaff, L. I., Carbon, 10, 165, 1972.

2.31   Hirano, S., Dechille, F. and Walker, P. L., J. High Temperature-High Pressures, 5, 207, 1973.

2.32   Whang, P. W., Dachille, F. and Walker, P. L., J. High Temperature-High Pressures, 6, 127,137, 1974.

2.33   Marsh, H., Dachille, F., Melvin, J. and Walker, P. L., Carbon, 9, 159, 1971.

2.34   Marsh, H., Foster, J. M., Hermon, G. and Iley, M., Fuel, 52, 234, 243, 253, 1973.

2.35   Fitzer, E. and Terwiesch, B., Carbon, 11, 570, 1973.

2.36   Hüttinger, K. J. and Rosenblatt, U., Proc. Fourth Conf. Ind. Carbon and Graphite, 1974, Soc. Chem. Ind., 1976, London, 50.

2.37   Hüttinger, K. J. and Rosenblatt, U., Carbon, 15, 69, 1977.

2.38   White, J. L., Air Force Report, No. SAMSO-TR-74-93, 1974.

2.39   Marsh, H., Fuel, 52, 205, 1973.

2.40   Singer, L. S. and Lewis, R. T., Abstructs of the 11th Biennial Conf. Carbon CG-27, 207, 1973, Gatlinburg.

2.41   Honda, H., Yamada, Y., Oi, S. and Fukuda, K., Extended Abstracts of the 11th Conf. Carbon, 219, 1973, Gatlinburg.

2.42   Kovac, C. A. and Lewis, I. C., Extended Abstracts of the 13th Conf. Carbon, 1977, 199, Irvine; Carbon, 16, 433, 1978.

2.43   Imamura, T., Yamada, Y., Oi, S and Honda, H., Carbon, 16, 281, 1978.

2.44   Hüttinger, K. J., Carbon, 72, 5, 1972.

2.45   Imamura, T. and Nakamizo, M., Carbon, 17, 207, 1979.

2.46   Imamura, T., Nakamizo, M. and Honada, H., Carbon, 16, 487, 1978.

2.47   Mochida, I., Miyasaka, H., Fujitsu, H. and Takeshita, K., Carbon, 15, 191, 1977.

2.48   Oberlin, A., Carbon, 22, 521, 1984.

2.49   Berkowitz, N. Symp. Sci. Technol. Coal, Dep. Energy, Mines resour., Ottawa, 149, 1967. Blayden, H. E. J. Chim. Phys. Spec., 15, 1969.

2.50   Blayden, H. E., Gibson, J. and Riley, H. L., Inst. of Fuel, War Time Bulletin, 250, 1945.

2.51   Hutcheon, J. M. and Jenkins, M. J., Second Conf. Ind. Carbon and Graphite, Soc. Chem. Ind., 433, 1966.

2.52   Kmetko, E. A., Proc. First and Second Conf. on Carbon, Buffalo, 21, 1953.

2.53   Dollimore, J. and Jenkins, M. J. Private Communication, 1966.

2.54   Labaton, V. Y., Jenkins, M. J. and Kilner, T., J. Chim. Phys. (special No.), 60, 1969.

2.55   Labaton, V. Y., Jenkins, M. J. and Kilner, T., U. K. A. E. A. TRG Report 1938(c).

CHAPTER III OPTICAL CRYSTALLOGRAPHY OF MESOPHASE

3.1 INTRODUCTION

The polarized-light technique provides a powerful tool to study the optical properties of transparent, translucent and opaque materials by using the polarized light. Polarized-light technique in recent years, has wide applications in Mineralogy, Metallurgy, Chemistry, Biology and in many branches of industrial technology. Various aspects of this technique have been described in details by a number of authors [1-6]. Marshall [4] and Dale [5] have discussed the optics of crystals. Hartshorne and Stuart [6] have given a good description for the microscopic examination of uniaxial and biaxial crystals under polarized-light.

3.2 POLARIZING MICROSCOPE

The polarizing microscope is essentially an ordinary compound microscope, with the difference that it has a revolving, graduated circular disc, a polarizing device below the stage, called the polarizer and a similar device above the objective, called the analyzer. The polarizer and analyzer may be referred to simply as the upper and lower polars and are made of calcite polarizing prisms, or "discs of polaroid".

Each polar transmits light wave vibrating in one direction only and for most purposes the polars are oriented so that their planes of vibration are mutually perpendicular or parallel.

The incident light passes through the polaroid disc, the polarizer, and is thus constrained to vibrate in one plane only. The polarizer can be rotated in its own plane and a second polaroid disc, the analyzer, is mounted in the body tube of the instrument. The analyzer can be rotated or withdrawn from the field of view to

enable a sample to be viewed in unpolarized light. When both the polarizer and analyzer are in the "crossed position", and they will not permit light to reach the eye piece so long as the medium between them is entirely isotropic. This is because light emerging from the polarizer is completely extinguished by the analyzer according to the law of Malus in optics.

There is a compensator or tint plate, inserted in the body tube of the instrument. The tint plate made of gypsum (also called first-order red plate) is placed at an angle of 45^0 to the vibration planes of the polarizer and the analyzer when they are in the crossed position.

The condensing lens system is situated between the rotating stage and the polarizer. Its primary function, as in the compound microscope, is to bring the incident light to a focus in the plane of the specimen.

The eye piece lens system, fitted to the microscope body is of the binocular type, having a X10 magnification. This together with the different objectives produces an overall magnification ranging from X25-X1000.

The illumination of the microscope is provided with 6V, 15W low-voltage halogen bulb. The bulb is contained in a well ventilated housing with a circular opening for the emission of light.

3.3 OPTICS OF CRYSTAL

While studying the propagation of light in crystal, Fresnel combined Maxwell's electro-magnetic equations and the general material equations which led to the

concept of the ordinary ray (O-ray) and extra ordinary ray (E-ray). These rays travel at different speeds in the crystal. A simple model based on the O-ray and E-ray could explain many of the phenomena observed in crystals.

When the basal section of a uniaxial crystal is viewed under the converging polarized beam of light, all the rays not travelling along the optic axis are doubly refracted [Fig.3.1]. At the upper surface there emerge at all points rays O and E derived from a given pair of incident parallel rays EE, which from there onwards travel along the same path, vibrating in planes at right angles to one another. One of these rays will have been retarded behind the other. When the retardation of one ray behind the other is exactly one wavelength or any whole number multiple of one wave length, brightness results due to interference. All emergent rays so allied to one another lie on the surfaces of an infinite number of geometrically similar cones coaxial with the optic axis [Fig.3.2] and the locus of their focal points in the interference figure in a circle. This gives rise to the series of concentric rings, called "isochrome" in the interference pattern [Fig.3.3]

The O-ray vibrates in the plane containing the ray and a line normal to both the ray and the optic axis, while an E-ray vibrates in the plane containing the ray and optic axis. The O-rays vibrate tangentially, and the E-rays radially. It is obvious that along the directions PP$'$ and AA$'$ which represent the vibration planes in the polarizer and analyzer respectively, extinction will result, and at 45^0 to these directions, between the dark rings, the interference figure will be most brightly illuminated. This pattern in the form of a maltese cross with characteristic isogyres is shown in Fig.3.3. In the central portion of the field, the rays are normal to the section and travel parallel to the optic axis and so the field remains dark there. The pattern in Fig.3.3 is a typical interference figure.

When rays of convergent light enter the section of a biaxial crystal not along the optic axis, double refraction takes place. Those rays the wave fronts of which travel along the optic axes are brought to a focus in the interference figure at two points called the "melatopes" which, being extinguished by the analyzer, appear dark. All other rays emerging from the crystal are made up of two components, differing in phase and vibrating in directions at right angles to one another (just as in the uniaxial case described before), and therefore resulting in interference in the analyzer. Emergent rays for which the retardation is the same lie on conical surfaces surrounding each optic axis, the sections of the cones being nearly circular when the inclination to the optic axes is small, and becoming more pear-shaped as this inclination increases; at still greater inclinations, the surfaces merge so as to surround both optic axes. The relative arrangement of representative surface corresponding to retardation's of λ, 2λ, 3λ, etc., for a given wavelength of light is illustrated in Fig.3.5. Each surface (together with its allied parallel surfaces) produces a ring of focal points in the interference figure similar in shape to its trace upon a horizontal plane. Such an interference figure consisting of two eyes or melatops surrounded by colored bands when viewed under white light is shown in Fig.3.6.

Absorption of one or more bands of wave length of the visible spectrum make the crystal appear colored. The intensity of light decreases as it penetrates more and more into the medium and the energy lost is converted into heat. In some crystals the frequency of the natural vibration of the electron system is same as that of light and a resonance effect takes place which compensates the absorption effect.

In anisotropic crystals, the two polarized components of a monochromatic rays are absorbed in different proportions. The same effect occurs for reflection as well.

This phenomenon is known as "pleochroism" which is one of the most important optical properties, studied by polarizing microscope.

Uniaxial crystals or fragments lying with their optic axes parallel to the axis of the microscope appear bright between crossed polars. The theory underlying the determination of sign in uniaxial optic-axis figures is easily grasped from the idea of double refraction of light waves entering and passing through the crystal plate. Light waves in each beam emerging from the crystal plate vibrate in the principal section and at right angles to the principal section. In Fig.3.4A light emerging at any point on the circle consists of two components: the extraordinary component E, containing waves in a plane the trace of which is a radial line; and the ordinary component O, containing waves vibrating in a plane the trace of which is tangent to the circle.

In positive crystals, waves in the extraordinary component are slower than waves in the ordinary component. In Fig.3.4B, the effects of the introduction of a first-order red plate on a diffuse optic-axis figures of a positive crystal are shown. The source of illumination is white light. In quadrants 2 and 4 (north-west and south-east) the trace of the vibration plane of the extraordinary component is parallel to the fast direction of the plate, and the red of the first-order red plate goes down in order to yellow. In the opposite quadrants (north-east and south-west) fast components in both the accessory plate and the crystal are parallel, and the color of the plate is elevated to blue. In white light, the area occupied by the isogyre assumes the interference color of the first-order red plate alone. In negative crystals, the effects of insertion of the first-order red plate are the opposite of those obtained from positive crystals.

3.4 BASIC PRINCIPLE OF A TINT PLATE

Tint plates or compensators are usually used to assist in the identification of interference colors. If the direction of the slot through the tubes is at 45^0 to the vibration direction of the polars in their crossed position then the compensators must be mounted so that one of its vibration direction is parallel to the plate when it is inserted. The basic principle of a tint plate is shown in Fig.3.7.

The most common compensators are (i) quarter wave mica plate (also called the quarter undulation plate), (ii) first-order red or unit-retardation plate (sometimes called the gypsum plate) and (iii) the simple quartz wedge.

The quarter-wave plate is made of a sheet of muscovite mica cleaved to such a thickness that one transmitted component is retarded a quarter of a wave of yellow light behind the other, i.e., by about 145nm. By itself between crossed polars the plate gives a pale gray interference color. The first-order red plate may be made of a cleavage sheet of gypsum. The thickness of this sheet is such that the relative retardation between the two transmitted components is one wavelength of yellow light (~575nm). Between crossed polars it gives violet to red interference color at the end of the first order and is usually called the first-order red or red I plate. It is also known as the sensitive red or sensitive tint plate because, if it suffers a very small subtractive effect, color is changed to orange or yellow, while if it suffers a very small additive effect the red color is raised to indigo or blue. In general, the first-order red plate is more suitable for specimen showing a very indistinct color since, owing to the sensitive color of the plate, additive and subtractive effects are sharply distinguished.

3.5 OPTICAL STUDIES OF THE CARBONACEOUS MESOPHASE SPHERES

Reflected polarized-light microscopy using crossed polarizers with a gypsum plate has been employed to investigate the microstructure of carbonaceous mesophase formed at the early stage of carbonization. It follows from the changes in pleochroism and isogyres occurring with the stage rotation, that a simple mesophase spherule is optically a uniaxial positive liquid crystal belonging to the hexagonal system with a straight extinction. Observations of changes in pleochroism and in extinction contours for coalesced and for deformed mesophas, permit to distinguish crosses from nodes and by that to identify four types of linear defects in the stacking of the aromatic layer planes.

The theoretical background for working with reflected polarized-light was provided largely with the help of the mathematical treatment by Drude [7]. This was followed by practical applications to microscopy initiated by Wright [8] who gave a summary of the theory, starting from the Maxwell's equations, which deals with the special cases of normal incidence on a surface normal to an optical symmetry plane. When the reflected light can be represented by two plane polarized components at right angles, subject to a phase difference, the cases were dealt with more directly by Woodrow, Mott and Haines [9].

A general remark of Taylor [10] concerning the reflectance pleochroism of carbons, coal and graphites has generally assumed that the reflected-light microscopy is analogous to the transmitted one. The fundamental equations for reflectance pleochroism have not been reviewed in the carbon literature since 1928 despite the predominance of the use of reflected-light microscopy technique. The

transmitted light microscopy observations of the mesophase spherules have in broad outline been related to the experiments of reflected light microscopy.

Observation of maltese cross-patterns has been made on pyrolytic carbon (PyC) deposit by Gray and Cathcart [11] when the microscope was in the orthoscopic mode and not on the conscopic mode. Fig.3.8 shows a schematic representation of a PVC-coated particle. The thin lines are the 'c' axes of the PVC fibres; in this case the 'c' axis coincides with the optic axis. When a beam of plane polarized light, incident normally on a hexagonal crystal, is reflected from a surface not perpendicular to the 'c' axis, the reflected beam is resolved into two components, R_s and R_p. The electric vectors of these two components vibrate in perpendicular and parallel directions respectively to the principal plane of the crystal (the principal plane is parallel to the 'c' axis). These can be expressed in terms of the incident vectors as follows

$$\underline{R}_p = \underline{E}_p \frac{(n_p - 1)}{(n_p + 1)}$$

$$\underline{R}_s = \underline{E}_s \frac{(n_s - 1)}{(n_s + 1)}$$

where n_p and n_s are the refractive indices parallel and perpendicular to the principal plane.

At the earliest stage, the spherical bodies are strongly pleochroic. Their absorption of plane-polarized light varies with orientation from being very strong (color almost black) to very weak (colorless or pale yellow). Analogous behavior is observed in reflected light. However, the pleochroism of the spherical bodies is not quite as

simple as that in pleochroic crystal. As the spherical bodies is not quit as simple as that in pleochroic crystal. As the spherical bodies grow larger it can be seen that the pleochroism is not uniform but that dark bars move across the sphere, unite, and then move out again [Fig.3.8]. Between crossed nicols, the spherical bodies, when small, behave essentially as single crystals, lightening and darkening four times per stage revolution. As the bodies grow larger the simple extinction gives way to the sequence shown in Fig.3.9.

Honda, Kimura and Sanada [12] employed the so-called 'sensitive tint technique' in an attempt to get further information about the structures. The changes in pleochroism and in extinction contours for the mesophase spherules are shown in Fig.3.10. They concluded that a simple mesophase spherules is optically a uniaxial positive liquid crystal belonging to the hexagonal system with a straight extinction.
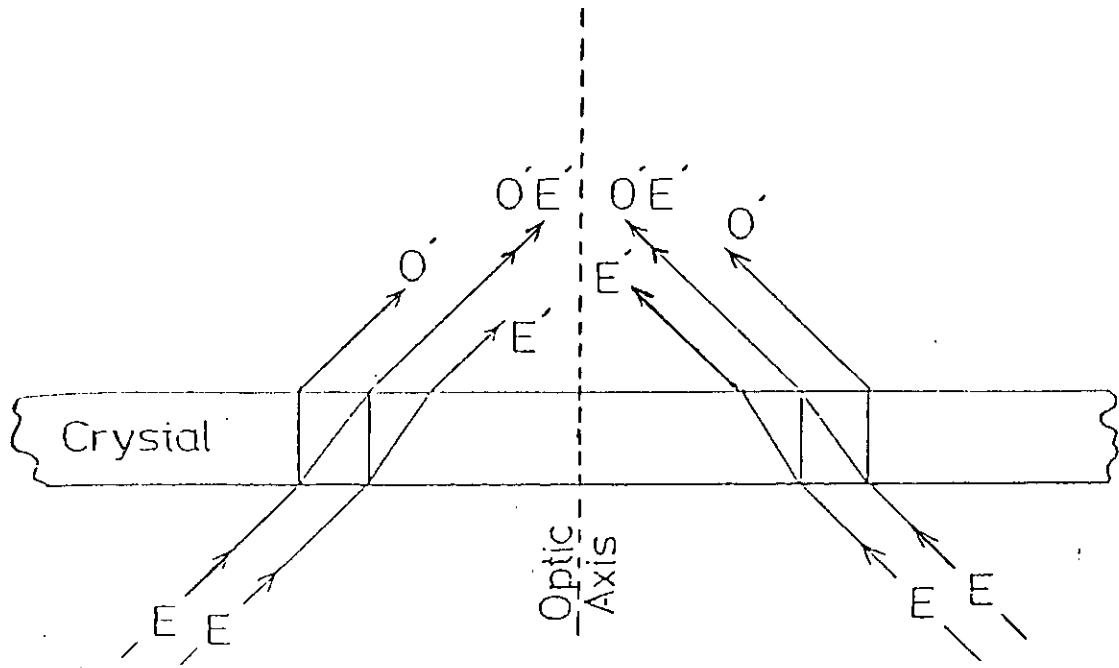
Fig 3.1   Passage of convergent polarized light through a uniaxial crystal
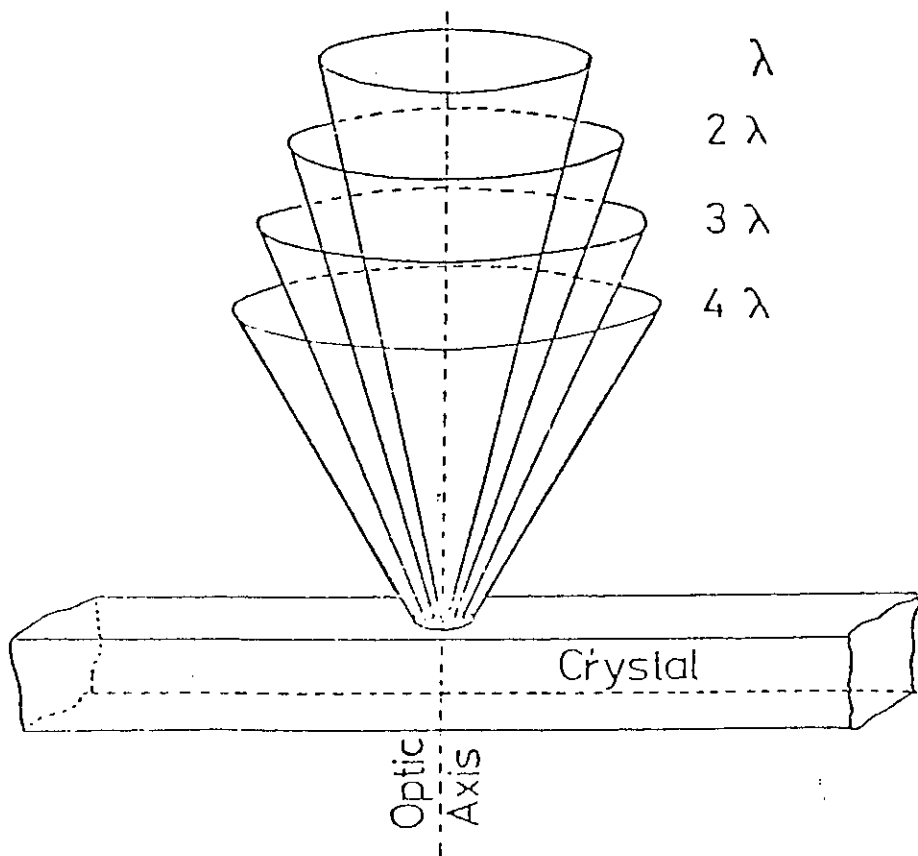normal to the optic axis.

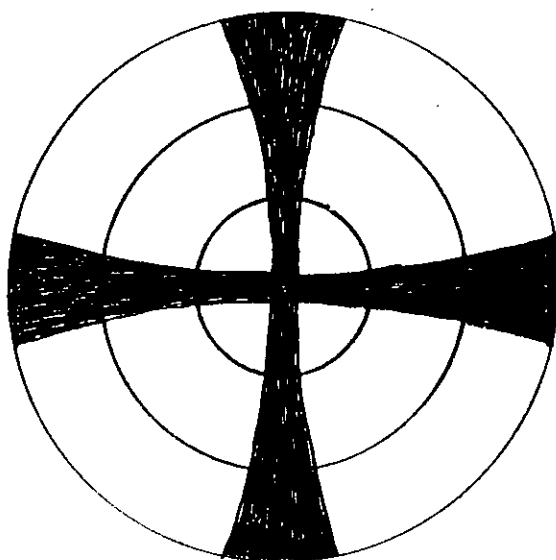Fig 3.2   Cones of equal retardation around the optic axis of a uniaxial crystal.

Fig 3.3   Typical interference figure for uniaxial crystal.
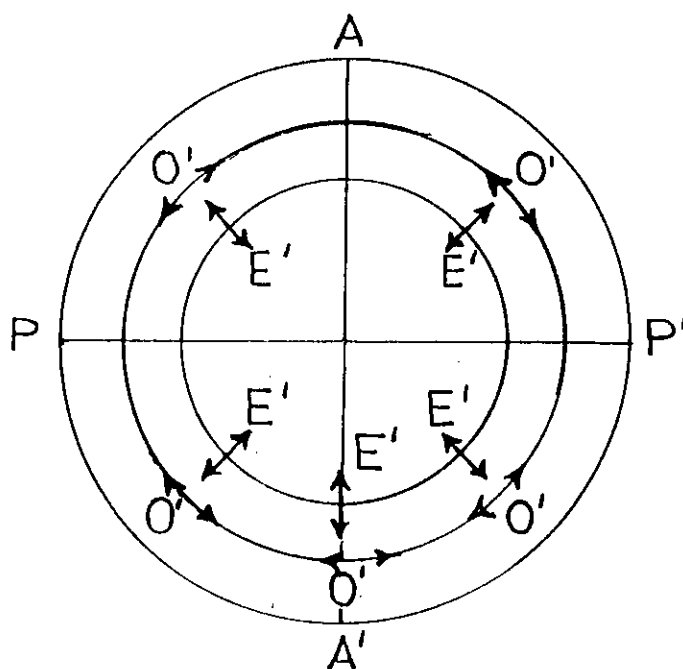
Fig 3.4A   Directions of vibration of O- and E-rays (AA', PP'- vibration planes in polarizer and analyzer).
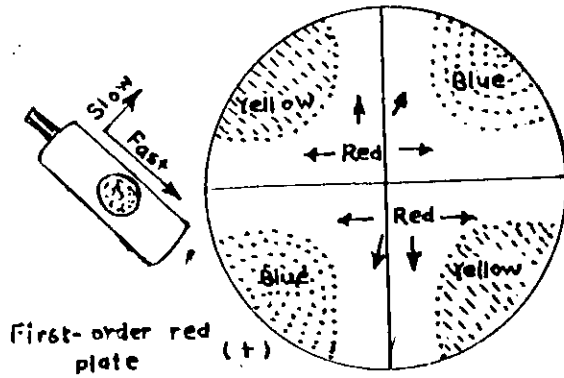
Fig 3.4B   Effect of introducing a first order red plate over a uniaxial optic axis figure.
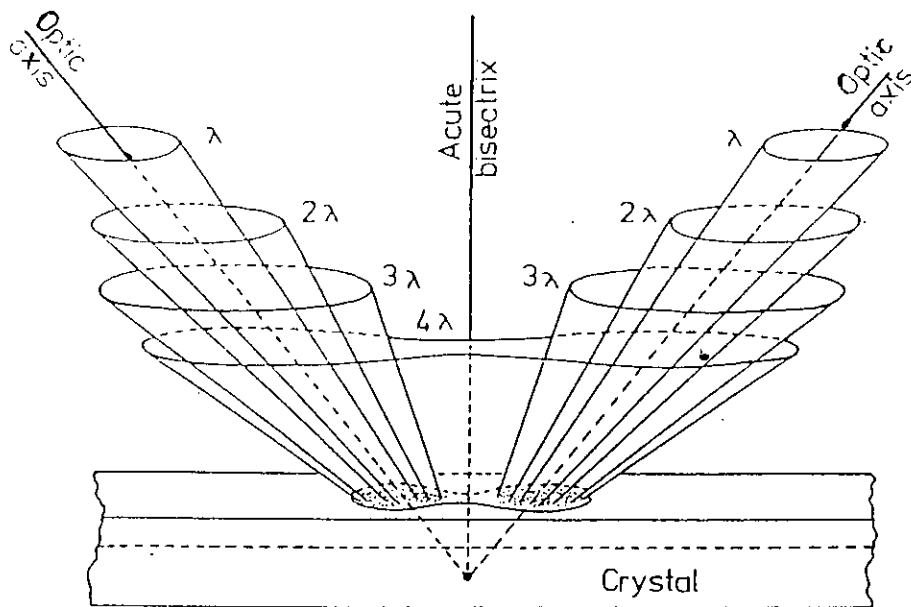
Fig 3.5   Surfaces of equal retardation around the optic axes of a biaxial crystal.

(a)
Extinction position

(b)
45° position
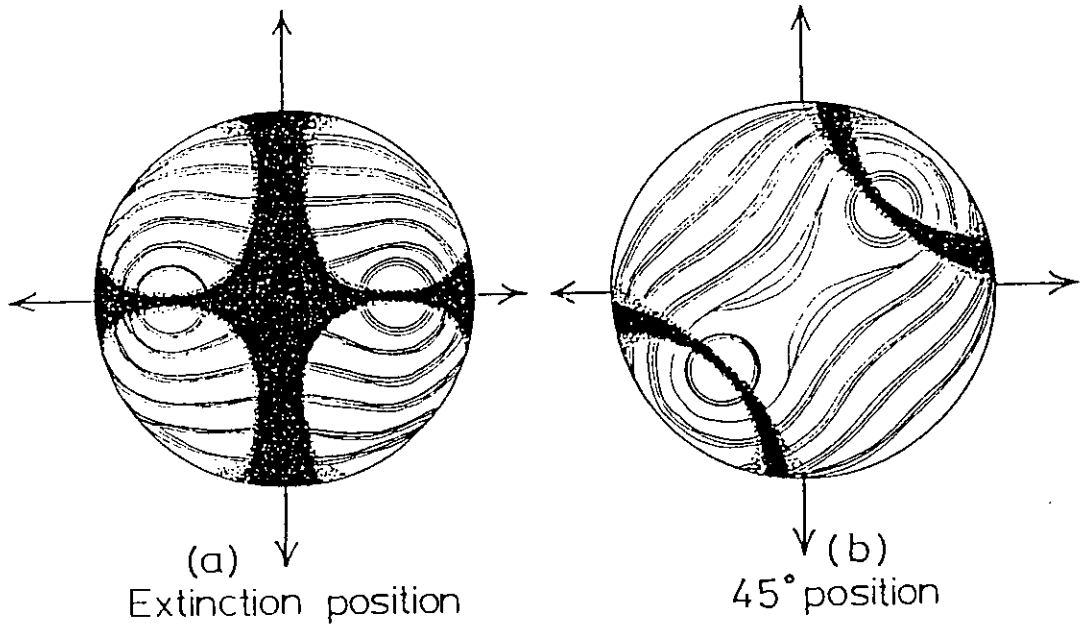
Fig 3.6   Biaxial interference figure given by a section normal to the acute bisectrix.
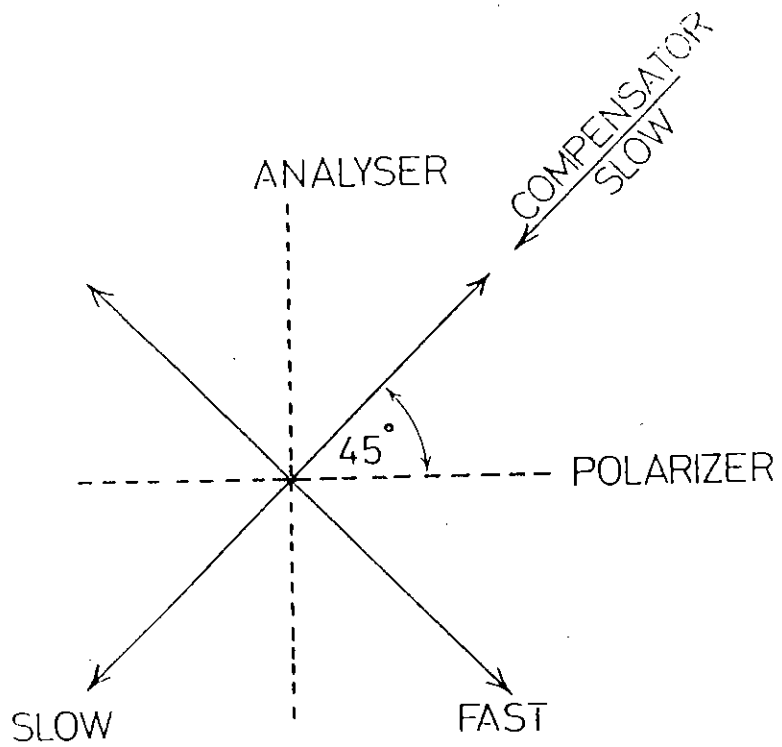
(A) additive effect : Coloured raised.
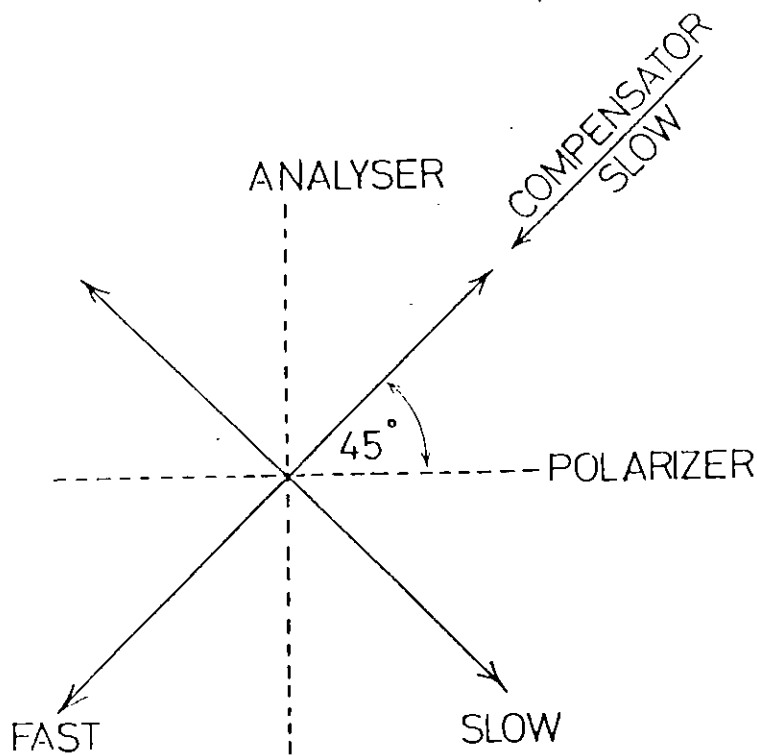
(B) subtractive effect : Coloured lowered

Figure 3.7   Basic principle of a tint plate.

Sense of stage rotation   Vibration direction of polarizer
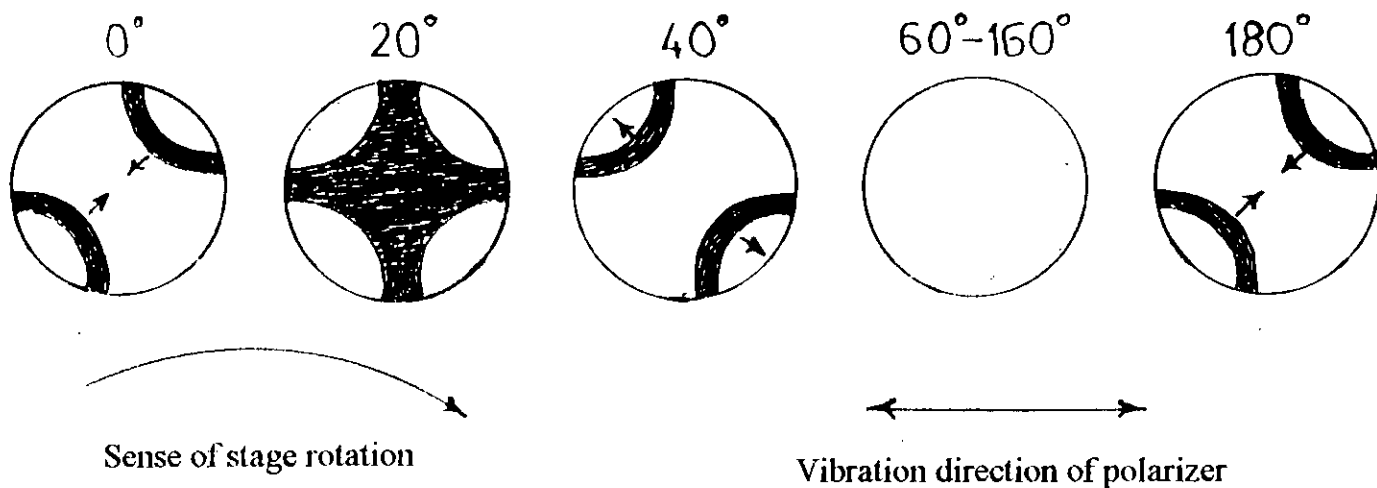
Fig 3.8   Pleochroic phenomena observed when symmetrically oriented spherical body is rotated with respect to plane of polarized light.

Sense of stage rotation

Vibration directions of polarizer and analyser
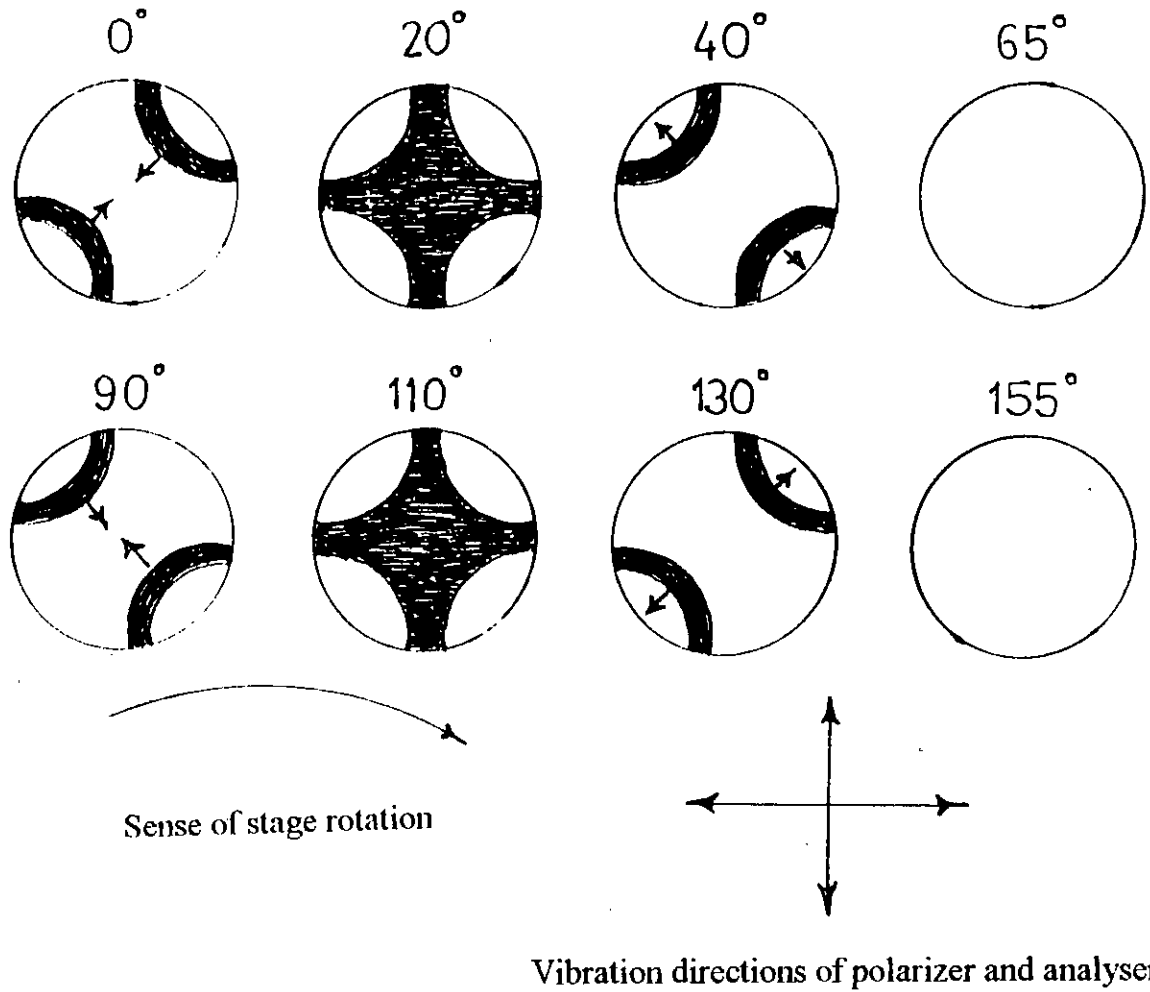
Fig 3.9   Phenomena observed when symmetrically oriented spherical body is rotated between crossed polars.

Extinction position

Diagonal position Subtraction

Sectioned exactly at its median plane containing C-axis (perpendicular to lamellae)

Addition

Sectioned above or below its median plane (parallel to lamellae)

0°   15°   30°   45°
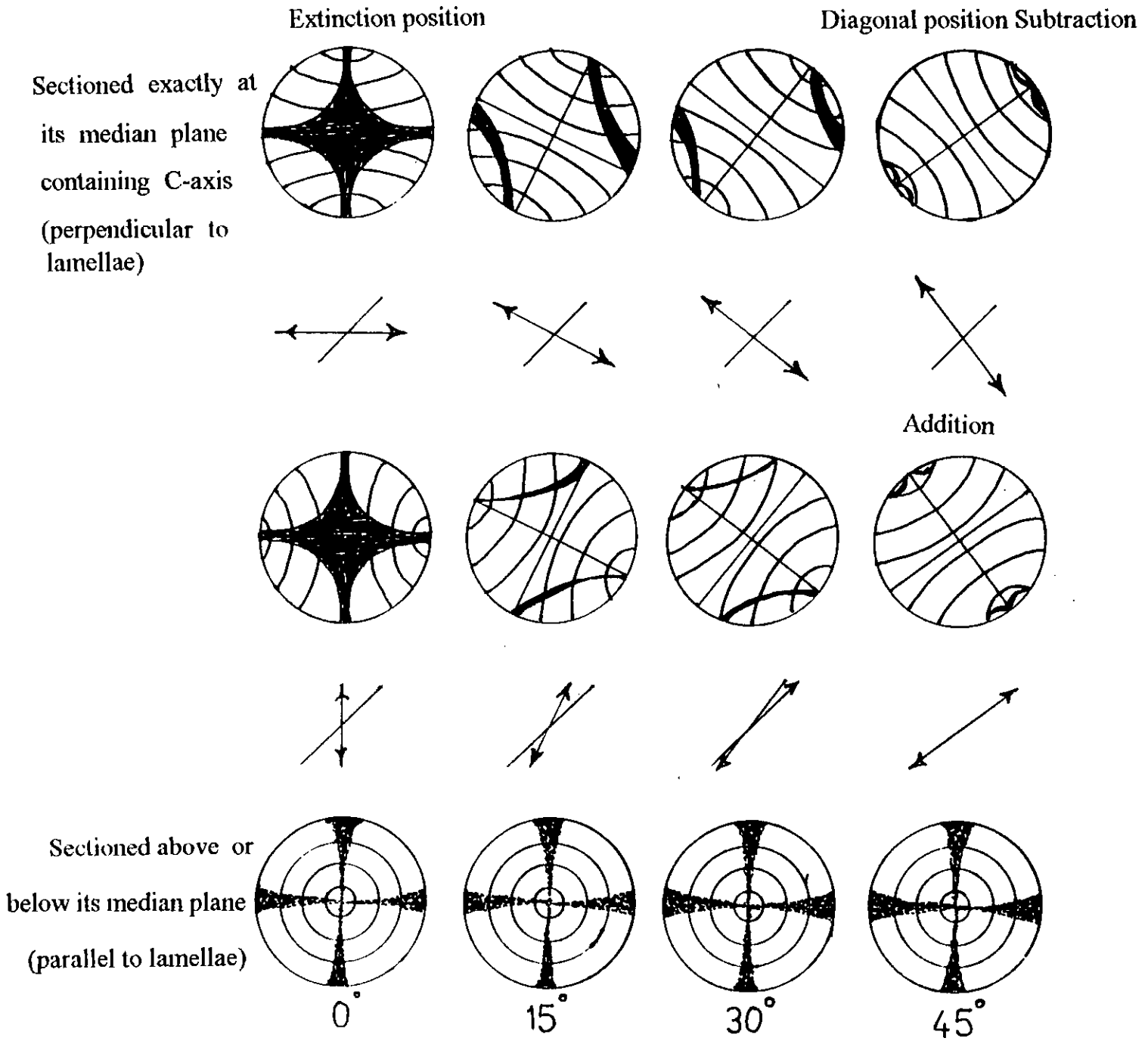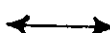
Fig 3.10   Schematic changes of pleochroism and of the extinction contours observed when mesophase spherules are rotated between crossed polarizers with a gypsum plate.

←——→ Vibration direction of extraordinary ray in mesophase spherule.

Vibration direction of extraordinary ray in gypsum plate.

REFERENCES

3.1   Hallimond, A. F., The Polarizing Microscope, Vickers Instrument, York, 1970.

3.2   Conn, G. K. T., and Bradshaw, F. J., Polarized Light in Metallography, Butterworths, London, 1952.

3.3   Mott, B.W., and Haines, H. R., J. Inst. Met, 80, 629, 1952.

3.4   Marshall, C. E., Introduction to Crystal Optics, Coke, Troughton and Simms, York, 1953.

3.5   Dale, A. B., The Form and Properties of Crystals, Cambridge University Press, London, 1932.

3.6   Hartshorne, N. H., and Stuart, A., Crystal and the Polarizing Microscope, Edward Arnold Ltd., London, 1970.

3.7   Drude, P., Ann. Phys. 32, 584, 1887.

3.8   Wright, F. E., Proc. Amer. Phil. Soc., 58, 401, 1919.

3.9   Woodrow, J., Mott, B. W. and Haines, H. R., Proc. Phys. Soc., 65, 603 1952.

3.10   Taylor, G. H., Fuel, 40, 465, 1961.

3.11   Gray, R. J., and Cathcart, J. V., J. Nuclear Materials, 19, 81, 1966.

3.12   Honda, H., Kimura, H., and Sanada, Y., Carbon, 9, 695, 1971.

CHAPTER IV EXPERIMENTAL DETAILS

4.1   INTRODUCTION

Experimental investigations performed for characterization of the pyrene sample and ultimately for determining their precursor states for graphitization are outlined below:

i)   Infrared (IR) Spectroscopic Study

Infrared spectroscopic study was done for identifying the structural changes of the sample during carbonization.

ii)   Differential Thermal Analysis (DTA)

Differential thermal analysis (DTA) was employed to locate the temperature region of mesophase transformation.

iii)   Thermogravimetric Analysis (TGA)

Thermogravimetric analysis (TGA) was carried out to calculate the dynamic weight loss of the sample during carbonization.

iv)   X-ray Diffractometric (XRD) Analysis

X-ray diffractometric analysis was carried out to determine the interlayer distances between the planes in the material pyrolyzed at different temperatures and different durations.

v)   Polarized-light Technique

The polarized light microscope was used to observe the mesophase microstructures.

4.2   SAMPLE

Any organic compound which undergoes substitution reactions of carbon-hydrogen (C-H) bonds is said to be aromatic. Generally, aromatic compounds are obtained by the distillation of coal-tar. Fused or condensed aromatic hydrocarbons contain more than one ring and have two carbons shared by two or three aromatic rings. The most important members of this class are naphthalene, anthracene and phenanthrene, etc.. Pyrene was taken as a higher aromatic compound in this work. High purity about 99% (supplied by "Tokyo Kasei Kogyo Co. Ltd.", Japan) analar grade was used. It melts at 149-151^{0}C and boils at 260°C. Its molecular weight is 202.26. It is a greenish yellow solid. Its formula is $C_{16}H_{10}$.
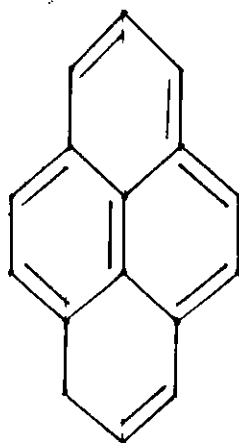
Structure of Pyrene ($C_{16}H_{10}$)

4.3 PYROLYSIS OF PYRENE

Pyrene was carbonized by sealed tube technique. Carbonization [1-6] was carried out using pyrex glass tubes in a locally manufactured solinoidal electric furnace having temperature limit up to 800°C [Fig.4.1].

The pyrex glass tube of 25cm in length, 1.6cm in an internal diameter having 0.15cm in wall thickness with the sample inside was sealed at both the ends . This sealed tube was then placed inside a steel bomb fitted with screw caps at both the ends, and the whole arrangement was carefully placed in a solenoidal furnace.

Pyrene was heated at 410^0C for different durations. During heating, the pressure inside the sealed tube increases primarily because of the evolution of H_2 and other hydrocarbon gases from the sample. After allowing the tube to cool to room temperature, it was opened inside a specially designed safety box [Fig.4.2] to avoid blast or blow, if any due to heavy pressure inside.

The safety box consists of a mechanical contrivance for cutting the sealed tube inside it with a diamond edge. The sealed tube containing the heat-treated sample was held inside the safety box at horizontal position and after cutting it in its central position with the diamond edge, a strong push was made on the cutting area from bottom, as a result of which the tube was found to open very easily. The heat-treated sample was then separated from the tube.

4.4 INFRARED (IR) SPECTROSCOPIC ANALYSIS

Infrared spectroscopic study provides valuable information concerning the structural information of organic substances. Generally there are five regions of absorption which can be related to the different modes of vibration of the aromatic system. These are (1) aromatic C-H stretching region, (2) Overtone region, (3)

aromatic ring (C=C) vibrations region, (4) in-plane bending region and (5) Out-of-plane bending region [7-9].

Summary of the characteristic absorption of aromatic ring systems

	Frequency (cm^{-1})	Remarks
1	3010-2860	C-H stretching
2	2000-1667	Overtone region
3	1618-1492	Aromatic ring (C=C) vibrations
4	1170-1040	C=H in-plane bending
5	900-690	=C-H out-of-plane bending

Pyrene was carbonized partially by heating to 410°C for 2, 4, & 6 hours' duration by sealed tube technique using a solenoidal tubular furnace described earlier in section 4.3. The resulting carbons were studied by infrared spectroscopic analysis. Samples were prepared by pressed-disc technique. The sample (1~5mg) was intimately mixed with approximately ~200mg of dry potassium Bromide powder. Mixing was effected by thorough grinding in a smooth agate mortar. The mixture is pressed with special dies under a pressure of 10,000-15,000 pounds per square inch to form a transparent disc. Potassium bromide pellets having 3mm in diameter were thus prepared to be used with a beam condenser. Infrared spectra of these samples were recorded in the wave number region 400-4000 cm^{-1} using IR-470 Shimadzu double beam spectrophotometer with its beam line 0, transmission expansion-5 and scan time 7 min. The instrument was calibrated for its accuracy with the spectra of a standard polystyrene film.

4.5   DIFFERENTIAL THERMAL ANALYSIS (DTA)

DTA is a process of accurately measuring the difference in the temperature between a thermocouple embedded to a sample and a thermocouple in a standard inert material such as aluminium oxide while both are being heated at a uniform rate. The technique of differential thermal analysis (DTA) is used to study the structural changes occurring both in solid and liquid materials under heat treatment. These changes may be due to dehydration, transition from one crystalline form to another, destruction of crystalline lattice, oxidation, decomposition, etc.. The principle of DTA consists of measuring heat changes associated with the physical or chemical changes occurring when any substance is gradually heated. This technique has recently attained considerable importance in determining the carbonizing and graphitizing properties of pure organic compounds, coals and pitches etc. [10-12].

When a sample and reference substance are heated or cooled at a constant rate under identical environment, their temperature differences are measured as a function of time or temperature (as shown by the curve in Fig.4.3b). The temperature of the reference substance, which is thermally inactive, rises uniformly when heated. The DTA method involves the simultaneous recording of temperature (T) which exists in the furnace and of the temperature difference (ΔT) which appears between the sample and thermally inert material (Fig. 4.3a). These differences of temperature arise due to the phase transitions or chemical reactions in the sample involving the evolution of heat (exothermic reaction) or absorption of heat (endothermic reaction). The exothermic and endothermic reactions are

52

generally shown in the DTA traces as positive and negative deviations respectively from a base line. So, DTA gives a continuous thermal record of reactions in a sample. The areas under the peaks are proportional to the amounts of active material present.

4.6 THERMOGRAVIMETRIC ANALYSIS (TGA)

The thermogravimetric analysis (TGA) involves the determination of weight loss from a sample as a function of time or temperature [$m=f(t$ or $T)$] while a sample is heated or cooled at a constant rate. This technique is effective for quantitative analysis of thermal reactions that are accompanied by mass changes due to release of volatile mater, evaporation, decomposition, gas absorption, desorption and dehydration etc [10,12]..

DTA & TGA APPARATUS

All DTA and TGA scans were carried out from room temperature to 1000°c under argon gas flow at the heating rate of 10°/min. DTA & TGA was performed using Thermal Analysis Station TAS 100, TG 8110, Thermoflex, Rigaku Corporation, Japan.

4.7 X-RAY DIFFRACTION (XRD)

X-ray diffraction study was performed to calculate the distances of interlayer spacing of the heat-treated carbonized samples. Pyrene was carbonized partially by

heating to $410^{0}C$ for 2, 4, 6 hours respectively and to $410°c$, $440°c$, $470°c$ for 6 hours each by sealed tube technique using solinoidal tabular furnace. The resulting carbons were studied by X-ray diffraction.

The samples were crushed into fine powder by using a pestle and mortar. Sample pested on a glass slide (area of 0.5X1) was then placed on the sample mounted in the diffractometer (Model No. JDX-8P, JEOL Co. Ltd., Tokyo, Japan). X-ray powder diffractograms were recorded using $CuK\alpha$ radiation with 30KV and current 30 mA.

Different diffraction patterns were obtained by using an automatic recorder. The parameters used for the identification of the sample is the spacing between the planes of atoms 'd' in the crystals.

Calculation of interplanar spacing

The Bragg equation for the nth order diffraction is written as:

$2d_{hkl}sin\theta = n\lambda,$

where, d_{hkl} is the interplanar spacing, θ is the angle of diffraction, λ is the wavelength of the X-ray radiation used for diffraction (i.e., $\lambda =1.5418$ A) and n is the number of order (here n=1) [13-16].

4.8   MICROGRAPHIC   PREPARATION   OF   SAMPLES   FOR MESOPHASE OBSERVATION

The micrographic preparation of the carbonaceous mesophase comprises the steps of impregnation, embedded in a cold-setting mounting resin, grinding, rough polishing and final polishing [1-6, 13-15].

Pyrolysed samples were mounted on epoxy resin. The mounted specimens were ground by silicon carbide papers, using tap water as lubricant and progressing from 120 to 600 grit. Light but steady pressures were applied while maintaining the same direction of grinding on each paper. Expected best results were obtained by using fresh paper for each specimen. After the final grinding on 600 grit paper, the surface of the specimen should appear bright independent of the level of heat treatment.

The process of rough and intermediate polishing were made in two stages on a wheel rotating about at 1500 rpm   (Matallographic specimens polisher, Type MSP-2) (Fig4.4) and covered with a TEXMET cloth. During each stage, the direction of polishing was maintained same. The specimen was not moved about the wheel but was only moved laterally between the center and the periphery. In the first stage, the polishing cloth was charged with Hyprez diamond compound of 3 μ size. Distilled water was used an lubricant, and relatively heavy pressures were applied. The specimen was thoroughly cleaned by water before undertaking the second stage in which the polishing cloth was charged with Hyprez-diamond compound of 1 μ size and relatively light pressure was applied as the polishing

advances. At the end of rough polishing, the characteristic mesophase microstructure was observed with crossed polarizers, although with many fine scratches still present.

Final polishing of the sample was carried out by high purity Linde Alpha Alumina powder. Powder was first mixed with distilled water and the sample was then rubbed gently by it with hand in the same direction for about ten minutes. When the final polishing was completed, the carbonaceous mesophase had a characteristic bright luster which proved the suitability for observation by the polarized-light microscopy.

4.9 POLARIZED-LIGHT MICROSCOPY AND OBSERVATION

The samples, after polishing with great care, were placed in turns on the stage of a Reichert-Jung, Astria, Nr. 369 013, Metabert Polarizing Microscope equipped with a 35mm Remica III photomicrographic camera and photographed by using reflected polarized light. Plate 4.5 shows a set up of a polarizing microscope. The light sources of the microscope was a 6V, 15W, halogen bulb. Fuji color films super HR100 were used. The colored mesophase spheres were produced by the insertion of a gypsum plate placed at an angle of 45^0 with one of the polars. The analyzer and polarizer remained crossed with respect to each other. This is the so-called Sensitive Tint Technique [4-6, 11]. An automatic exposure time was programmed depending on the intensity of reflected light. Exposure time was varied by using the various speed of films. The value of ASA-DIN was reduced to one-fourth, one-eighth of the original value of the film in the autocontrolled system for having better results. A suitable area of each specimen was photographed.
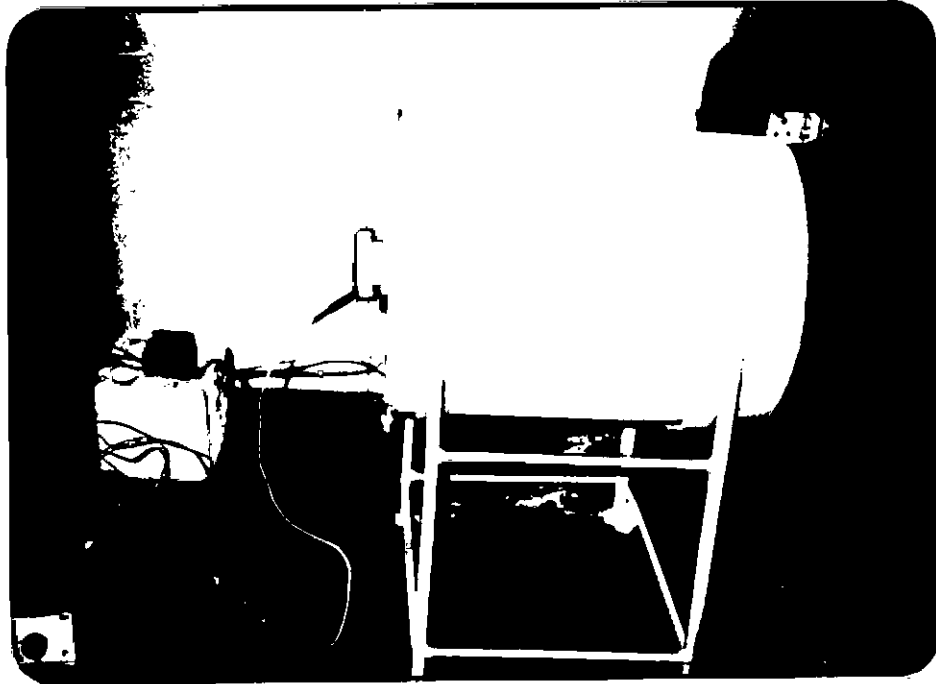
Fig 4.1 Locally manufactured solinoidal electric furnace.

Fig 4.2   Specially designed safety box.

REFERENCE CUP WITH
ANHYDROUS ALUMINA
MATCHED SAMPLE CUP

CERAMIC CENTERING
RING AND GAS DIFFUSER

PORCELAIN TUBE

RUBBER STOPPER

CERAMIC GAS INLET TUBE

T ref

ΔT

DIFFERENTIAL
THERMOCOUPLE
CHROMEL   LEADS

CHROMEL

ALUMEL

Fig 4.3a   DTA thermocouple assembly

Furnace
atmosphere
control

Furnace
controller

Furnace

S M R   Sample block

Gas   Vacuum

dc
Amplifier

X

Y

X–Y Recorder

Fig 4.3b   Block diagram of a differential thermal analysis equipment, (S) sample
thermocouple, (R) reference thermocouple, (M) monitor thermocouple.

Fig 4.4   Matallographic specimens polisher

Fig 4.5   Polarizing Microscope.

REFERENCES

4.1   Dubois, J., Agache, C., and White, J. L., Metallography, 3, 337-369, 1970.

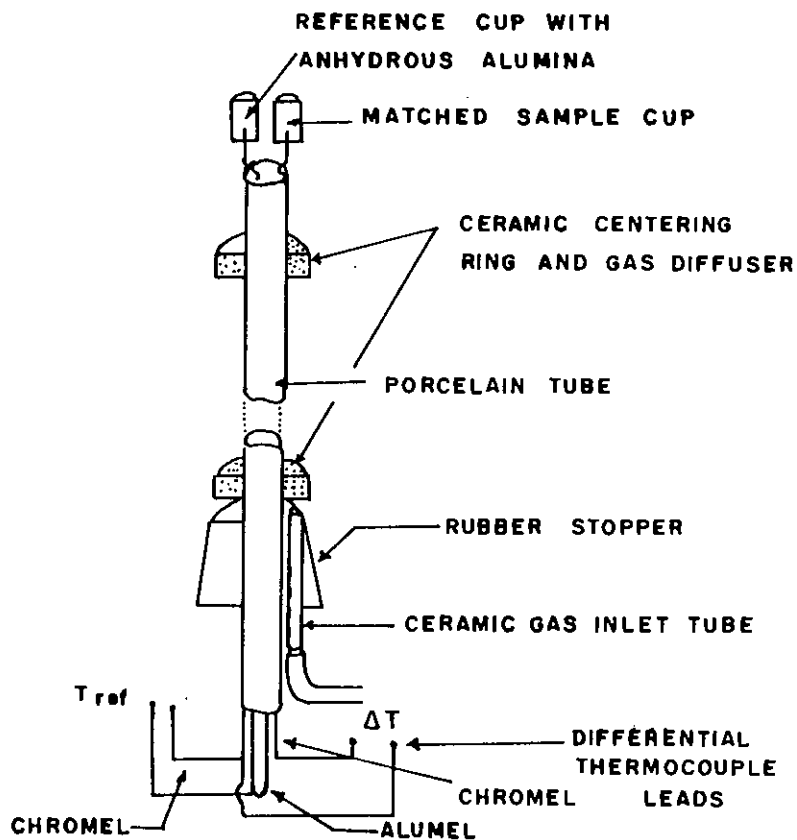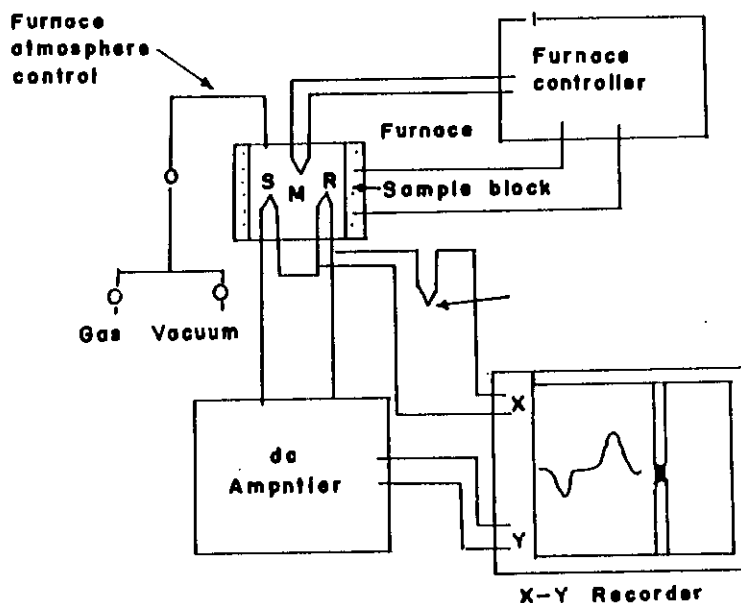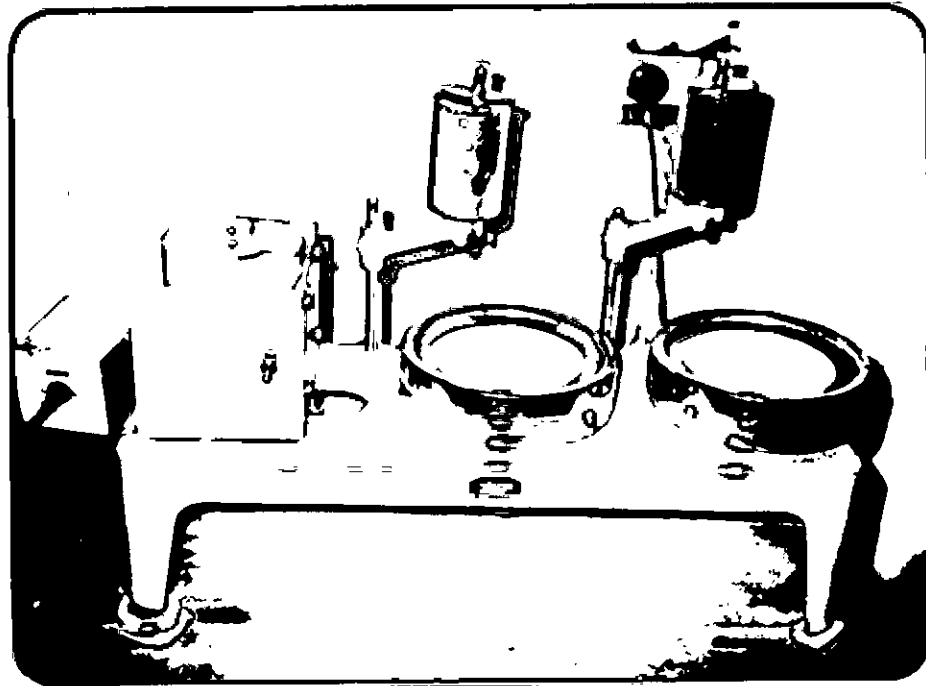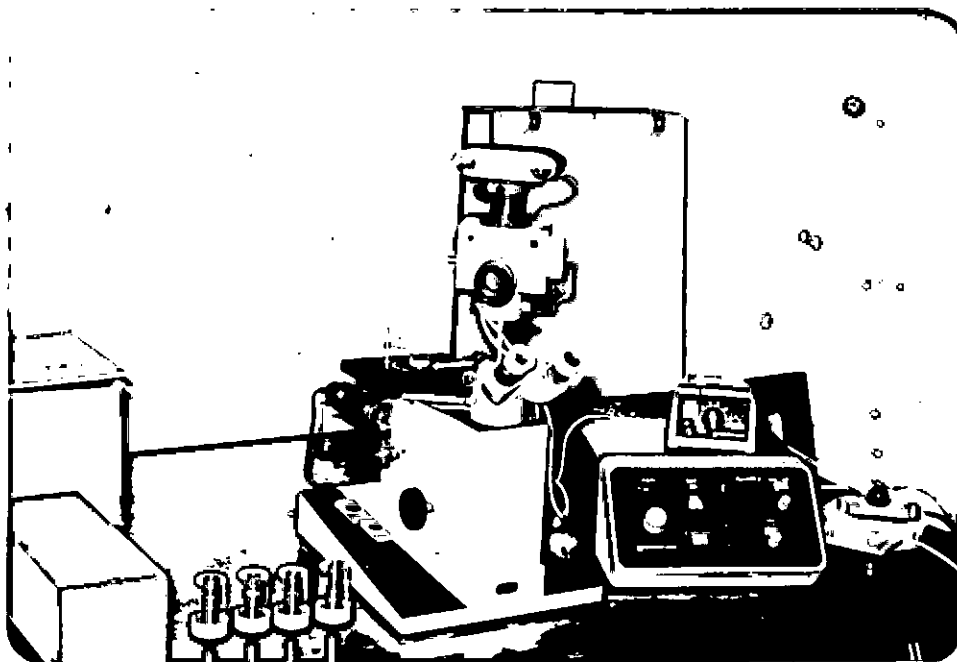4.2   John, J. M., and Richard, M. R., Industrial and Engineering Chemistry, 2, 237, 1958.

4.3   Kinney, C. R., The Chemistry of Petrolium Hydrocarbons, 113-136.

4.4   Brooks, J. D. and Taylor, G. H., Carbon, 3, 185, 1965.

4.5   Brooks, J. D. and Taylor, G. H., Chemistry and Physics of Carbon, 4, 243, 1968.

4.6   Kinney, C. R. and Delbel, E., Industrial and Engineering Chemistry, 46, 546, 1954.

4.7   Islam, O., Bhuiyan, A. H., and Ahmed, S., Thin Solid Films, 238, 191-194, 1994.

4.8   Silverstein, R. M., Bassler, G. C., and Morril, T. C., Spectrometric Identification of Organic Compounds, John Willey & Sons., NY, 1981.

4.9   Robeot, T. C., Infrared Spectrocopy, 2nd Edition, 1975.

4.10   Rashid, M. A., Hossain, T. and Asgar, M. A., Thermochimica Acta, 259, 263-268, 1995.

4.11   Lapina, N. A., Ostrovskii, V. S., and Kamenskii, I. V., Vysokomol Soyed., AII, 2073, 1969 (Translated in Polymer Science USSR, 11, 2367, 1969.

4.12   Oberlin, A., Carbon, 22, 521, 1984.

4.13   Hossain, T., and Dollimore, J., Thermochimica, Acta, 108, 211, 1986.

4.14   Jahan, S. T. and Hossain, T., Phy. Tea., Indian Phy. Soc., 2, 101, 1987.

4.15   Hossain, T. and Podder, J., Thermochimica Acta, 137, 225, 1989.

4.16   Sexena, B. S., Gupta, R. C., and Saxena, P. N., Fundamentals of Solid State Physics.

CHAPTER V   EXPERIMENTAL RESULTS AND DISCUSSION

5.1 INTRODUCTION

The importance of the formation of the carbonaceous mesophase as a precursor to graphitization has been discussed previously [Sec.2.7]. The structural changes of the samples during carbonization have been studied by Infrared spectroscopy. The temperature region of mesophase formation has been located by the Differential thermal analysis. The dynamic weight loss of the sample during carbonization has been carried out by the Thermogravimetric analysis. The interlayer distances of the carbonized sample for its graphitization have been carried out by the X-ray diffraction analysis. In the present study the mesophase formation has been examined and polarized-light photomicrographs of the various samples during mesophase formation have been taken in order to study the nucleation, growth and coalescence processes of the mesophase spherules at different heat-treatment temperatures.

5.2 INFRARED SPECTROSCOPY (IR)

Figure 5.1 shows the IR spectra of raw sample and partially carbonized samples for different heat treatment durations. The IR spectra of pyrene (raw sample) and heat- treated at $410^{0}C$ for 2, 4and 6 hours are represented by spectra A, B, C & D respectively in Fig.5.1.

The spectrum A in Fig.5.1 is well matched but with a few extra bands to the standard IR spectrum of pyrene. The absorption bands at $3010\text{-}2860\text{cm}^{-1}$ correspond to aromatic C-H neat together with a CH_3 (aliphatic) stretching vibrations; band at $2000\text{-}1667\text{cm}^{-1}$ arises from overtones or a combination band pattern of a meta-substituted aromatic structure; band at $1618\text{-}1492\text{cm}^{-1}$ forms a

ring C=C stretch; band at 1170-1040cm^{-1} indicate C=H in-plane bending and band at 900-690cm^{-1} indicate =C-H out-of-plane bending respectively.

The IR spectrum B, C & D (Fig.5.1) reveals a noticeable modification that all the absorption bands arises at the same region but intensity of the peaks decreases with increasing amount of heat. This is an indication of the modification to the pyrene structure on heat treatment. The band 900-675 cm^{-1} is attributed to the "aromatic band" i.e., aromaticity of the pyrene. These bands are mainly due to aromatic HCC (Hydrogen-Carbon-Carbon) rocking variations in aromatic and condensed aromatic ring systems. The higher intensities at 900-675cm^{-1} shows the higher aromaticity of pyrene.

5.3   DIFFERENTIAL THERMAL ANALYSIS AND THERMOGRA-VIMETRIC ANALYSIS

Differential thermal analysis (DTA) traces of the sample at different heat-treatment duration are presented in Fig.5.2. The main characteristics of these curves are the presence of a initial large endotherm at 151^{0}C due to melting of the tarry substance and the second large endotherm at 260^{0}C corresponds to the boiling point of the substance. These melting and boiling points are very close to the theoretical values.

The DTA curves show that the initial large endotherm gradually increases in size with the increasing duration of heat-treatment. This increase in the initial large endotherm indicates an increase in the heat of fusion, which in turn indicates the consequent increase of activation energy [10,11] and hence of graphitizing power.

The TGA curves of the same samples are presented in Fig.5.3. The weight losses of the samples start from $\simeq 100^{0}$C and substantially continue up to 353^{0}C and this amount of losses ($\simeq 45\text{-}55\%$) occurs, owing to the elimination of hydrogen and hydrocarbon gases. The TGA results show that the carbon yield is increased by the increasing pyrolysis temperature [11].

In preparing graphitizing carbon, it appears that under low temperature carbonization of polynuclear aromatic compound, carbon yield is usually increased. This indicates the increase of the magnitude of the graphitization [12]. For pyrene the highest carbon yield is observed than the other lower aromatic ring compounds like benzene, anthracene, phenanthrene under the same heat-treatment temperature and duration [Table 7]. The carbon yield virsus duration of heat-treatment for different aromatic ring compounds are shown in Fig 5.4.

5.4 X-RAY DIFFRACTION ANALYSIS

In the graphitic carbon, the extent of ordering that is associated with increasing order of graphitization can be estimated from x-ray diffraction pattern. With increasing carbonization, the interplanar spacing of carbon hexagonal planes decreases and approaches a regular crystalline structure to that of graphite. Fig.5.5 shows the diffraction patterns of raw and partially carbonized samples heat-treated at 410^{0}C for 2, 4 & 6 hours and are represented by a, b, c & d respectively. Fig. 5.5 shows an increase in sharpness of the diffraction lines with increasing carbonization. The interlayer distances of different samples, calculated from Fig.5.5 are depicted in table 1 to 4. It is seen that the interplanar distance decreases with increasing heat-treatment temperature (HTT) duration. Fig. 5.6 shows the diffraction patterns of raw and partially carbonized samples heat-treated

at 410°C, 440°C, 470°C for 6 hours and are represented by a, b, c & d respectively. The interlayer distances are depicted in table 4 to 6. No remarkable differences in results are found in the above two cases.

The interlayer spacing between the haxagonal lamellea structure is found to decrease with increasing heat-treatment temperatures at the same duration for the different aromatic ring compounds. The results of the changes of interlayer spacing is shown in table 8 [14]. It is obvious from the table 8 that for the same heat-treatment temperature and time, the decrease of d-spacing is more in pyrene than that of Anthracene. That is for the pyrene sample, the rate of change of d-spacing is increased compared to Anthracene. This clearly indicates that the degree of graphitization increases in the case of pyrene.

5.5 POLARIZED-LIGHT PHOTOMICROGRAPHS

The importance of the formation of carbonaceous mesophase as a precursor to graphitization has been discussed earlier in chapter 1. In the present study, the polarized-light photomicrographs of samples during mesophase formation have been examined by the polarized light technique in order to study the nucleation, growth and coalescence processes of the mesophase spherules developed at different heat -treatment temperatures.

Color photomicrographs of selected mesophase spheres of subsequent heat-treated samples are presented in plates 5.7a to 5.7d. Mesophase spherules start to appear at 430°c (plate 5.7a). There after they start to coalesce forming larger spherules at a higher temperature. Plate 5.7b shows the picture of such a coalescence at 435°C. At still higher temperature, the growing mesophase spherules coalesce to form

relatively complex bulk mesophase at 440°C. This is exhibited in plates 5.7c. Complete coalescence takes place to form a mosaic pattern at 445°C (plate 5.7d).

The growth of spherical unit bodies, their coalesced structures, mosaic and flow type mosaic are the essential features for the evidence of graphitizing carbon.

The temperature intervals of mesophase transition of higher aromatic ring compounds [19,20] is becoming shorter, as shown in table 5.9. This relatively shorter the mesophase transition predicts that the anisotropic crystallites structure is formed within that small range of temperature. The more the growth of the anisotropic crystallites within the smaller interval of mesophase transition, the more will be the magnitude of graphitization.
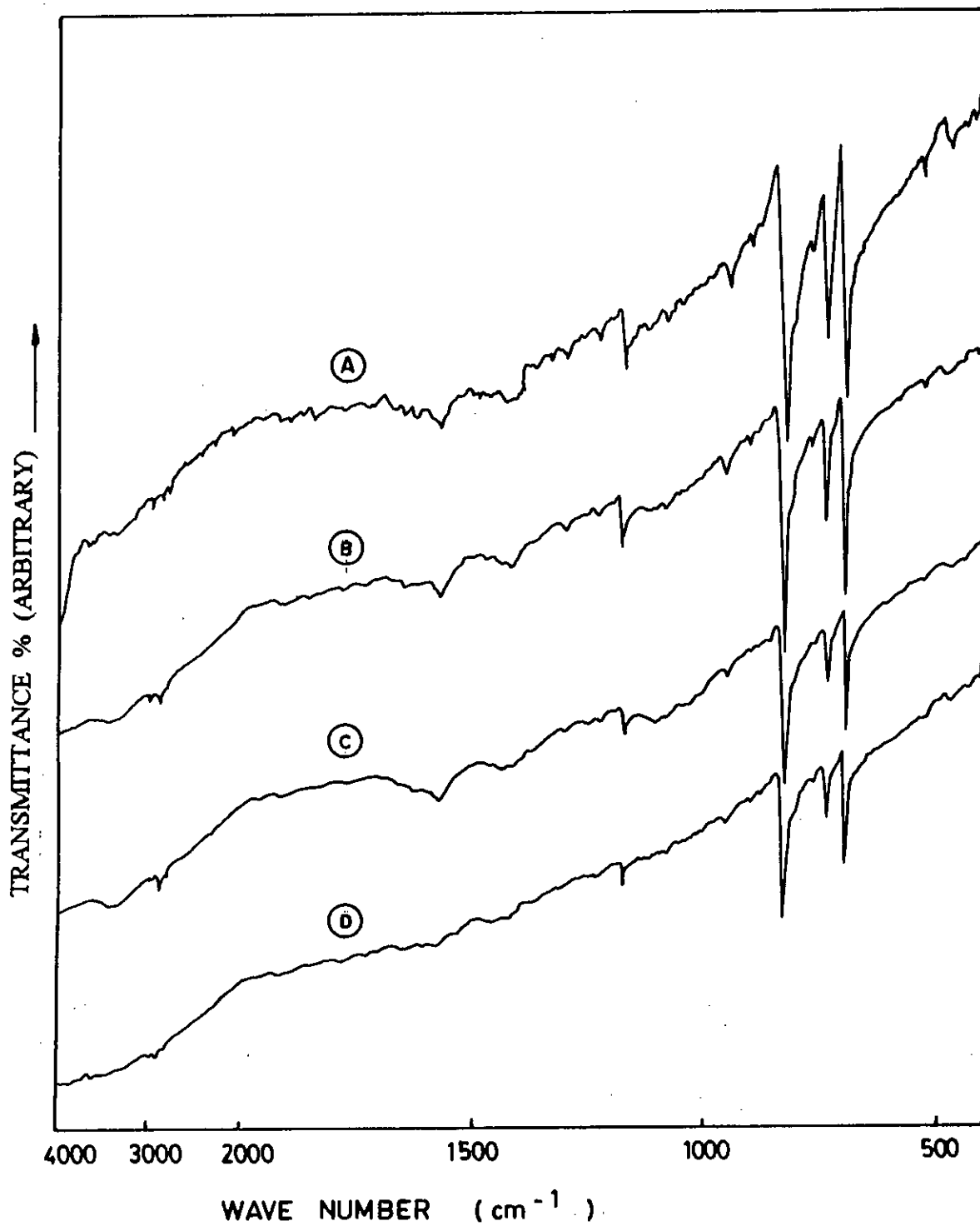
Fig 5.1   IR spectra (A) Pyrene (raw sample), (B) $410^{0}C$ for 2 hours, (C)
$410^{0}C$ for 4 hours, (D) $410^{0}C$ for 6 hours.
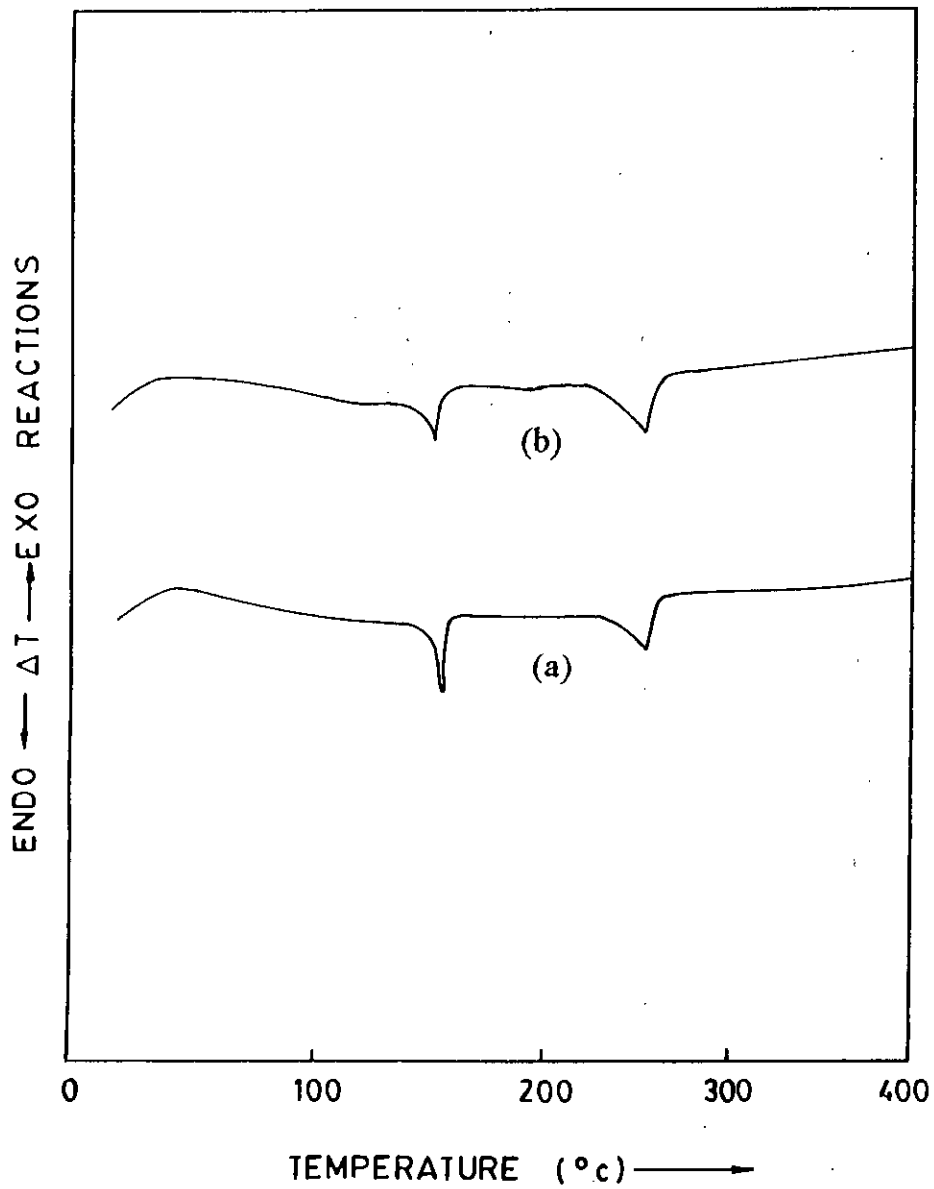
Fig 5.2   DTA traces (a) 410°C for 2 hours, (b) 410°C for 4 hours.
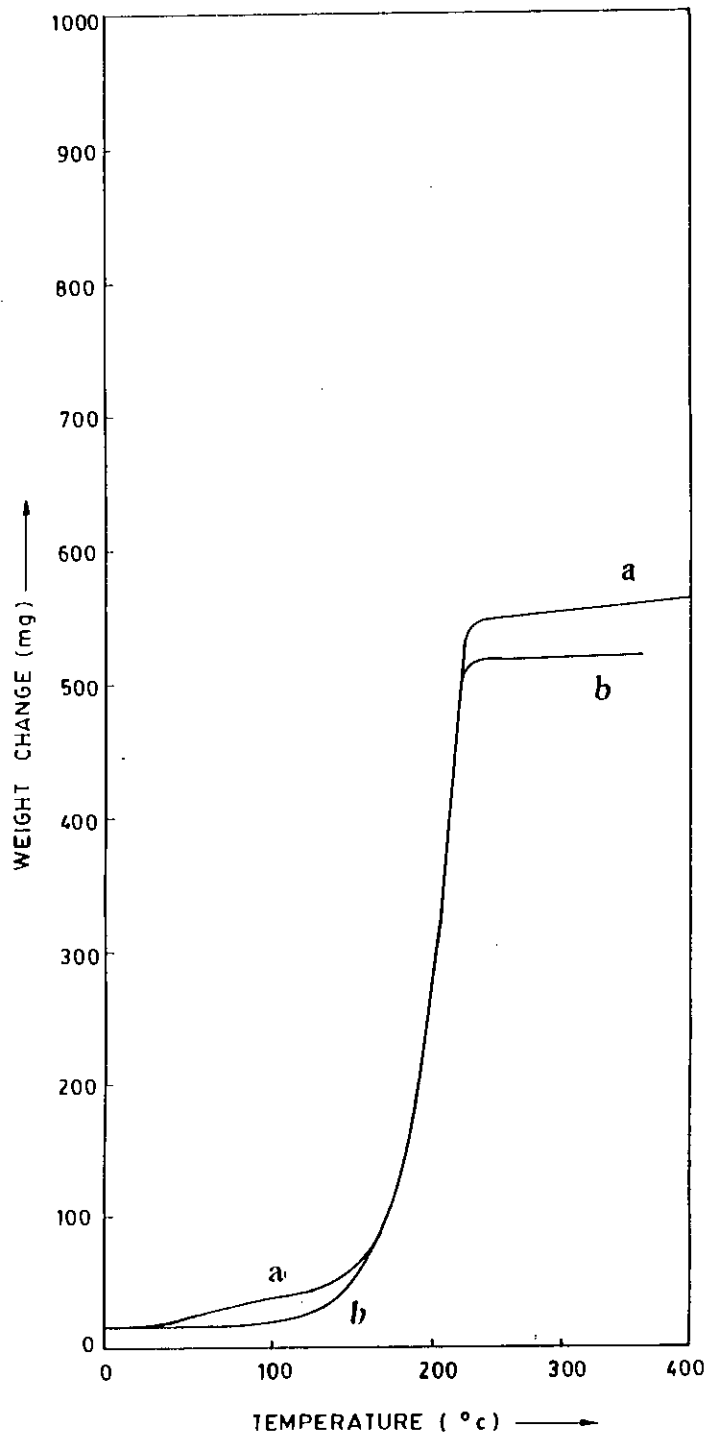
Fig 5.3   TGA curves (a) 410^0C for 2 hours, (b) 410^0C for 4 hours.
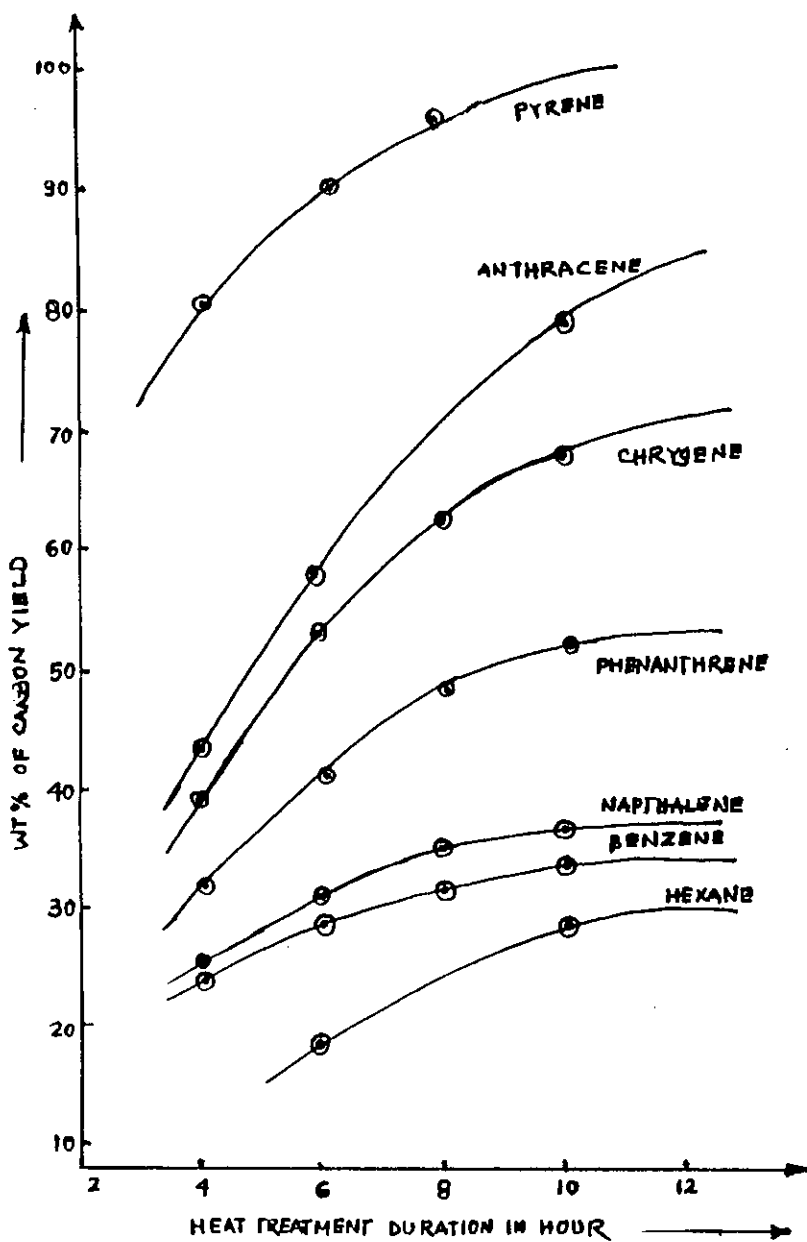
Fig 5.4   Percentage of carbon yield at 500^0C for different heat-treatment
duration
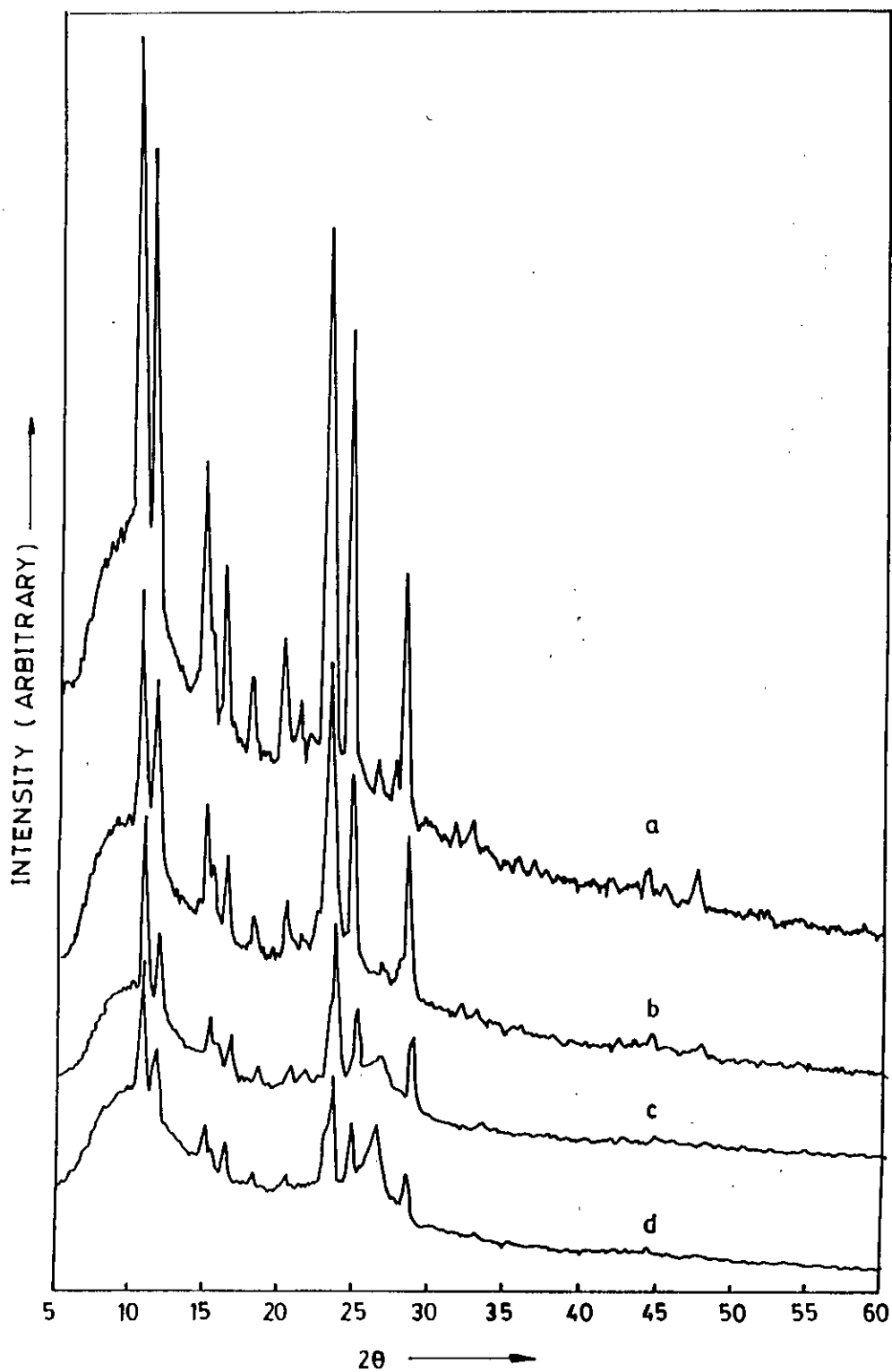
Fig 5.5   X-ray diffraction pattern (a) Pyrene (raw sample), (b) 410^0C for 2

hours, (c) 410^0C for 4 hours, (d) 410^0C for 6 hours.
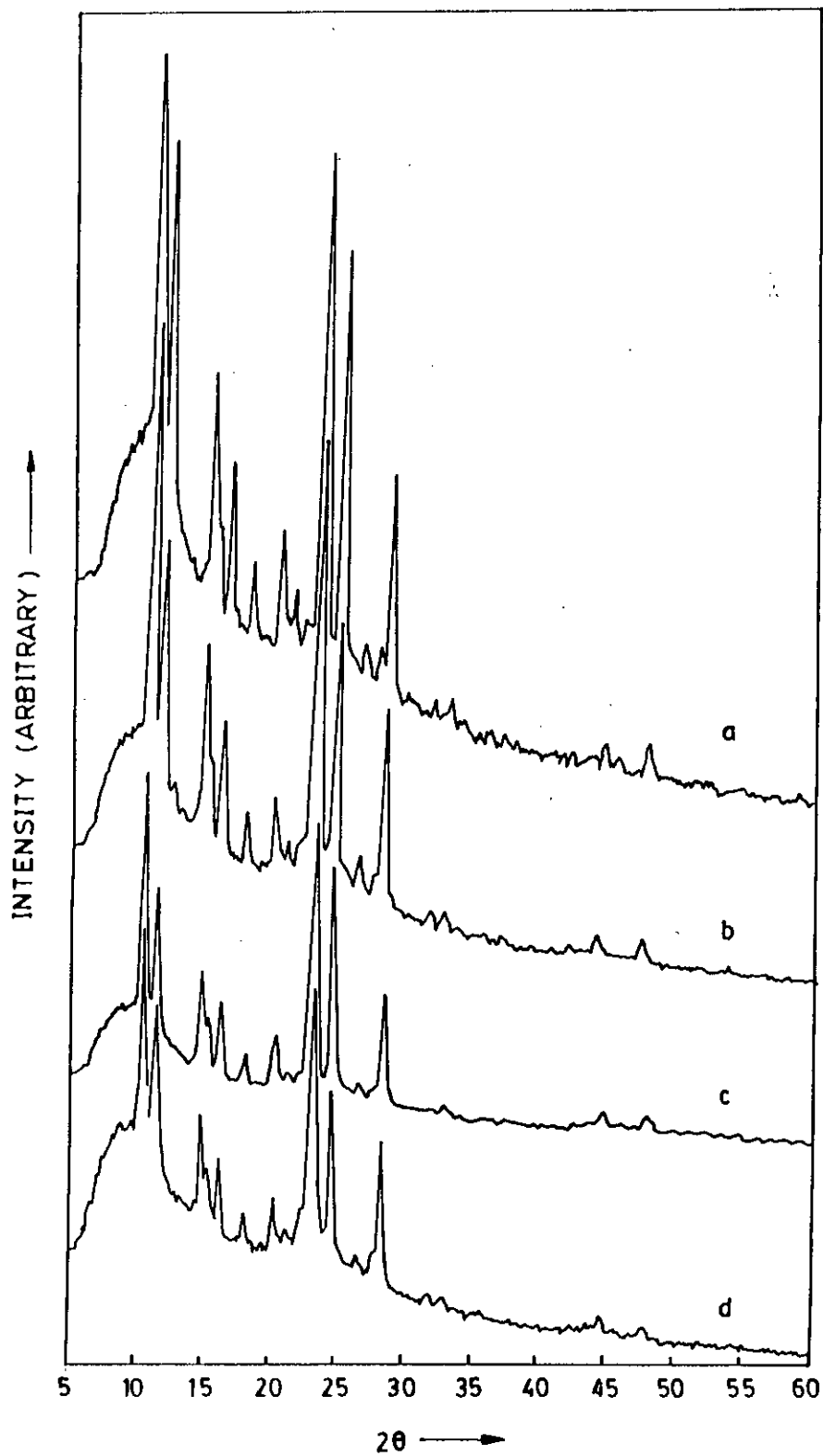
Fig 5.6   X-ray diffraction pattern (a) Pyrene (raw sample), (b) 410^0C for 6

hours, (c) 440^0C for 6 hours, (d) 470^0C for 6 hours.
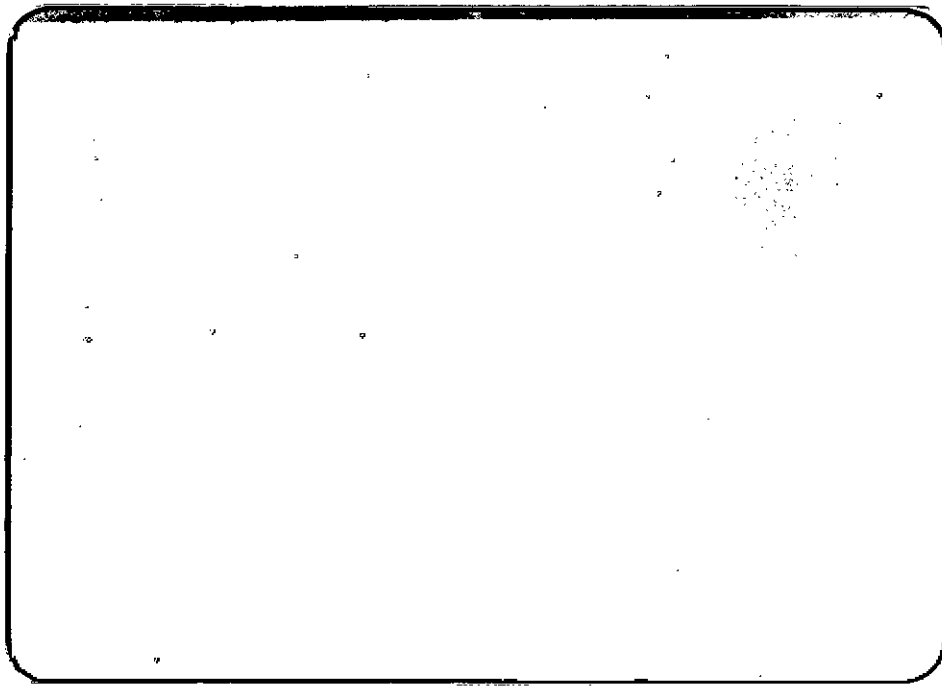
Fig 5.7a Formation of mesophase spherule on heat-treated at $430^{0}C$ for 5

hours.
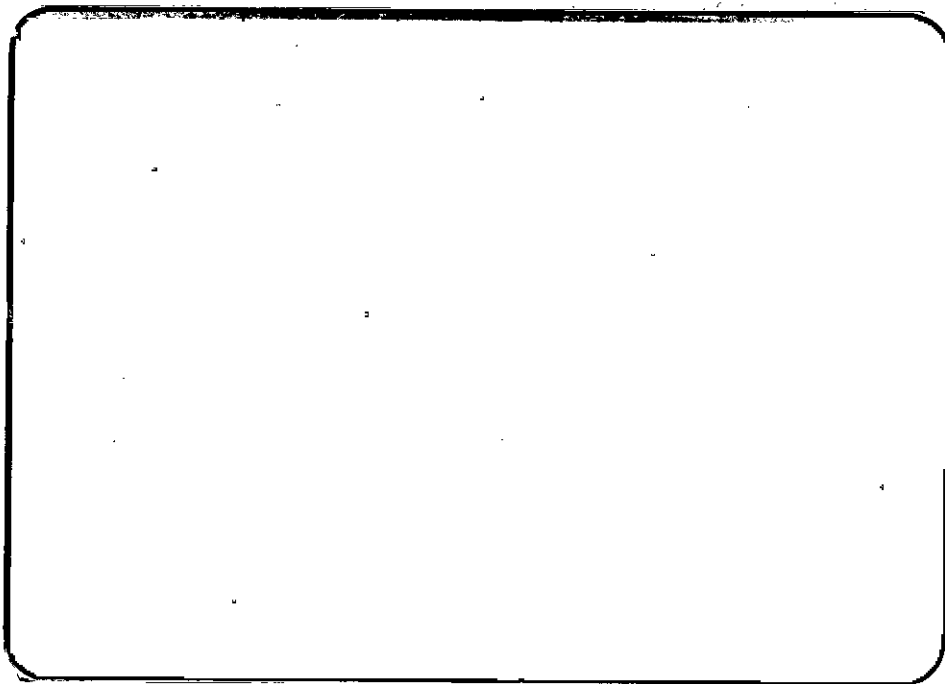
Fig 5.7b Formation of large mesophase spherule on heat-treated at $435^{0}C$ for 5

hours
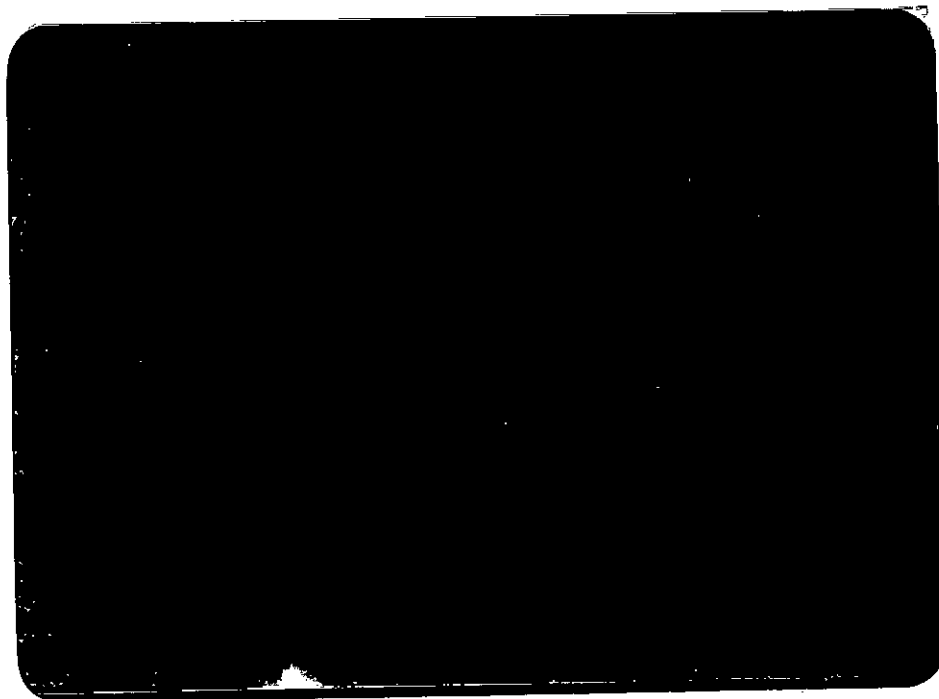
Fig 5.7c   Mesophase spherule in coalescence on heat-treatment at 440^{0}C for 5
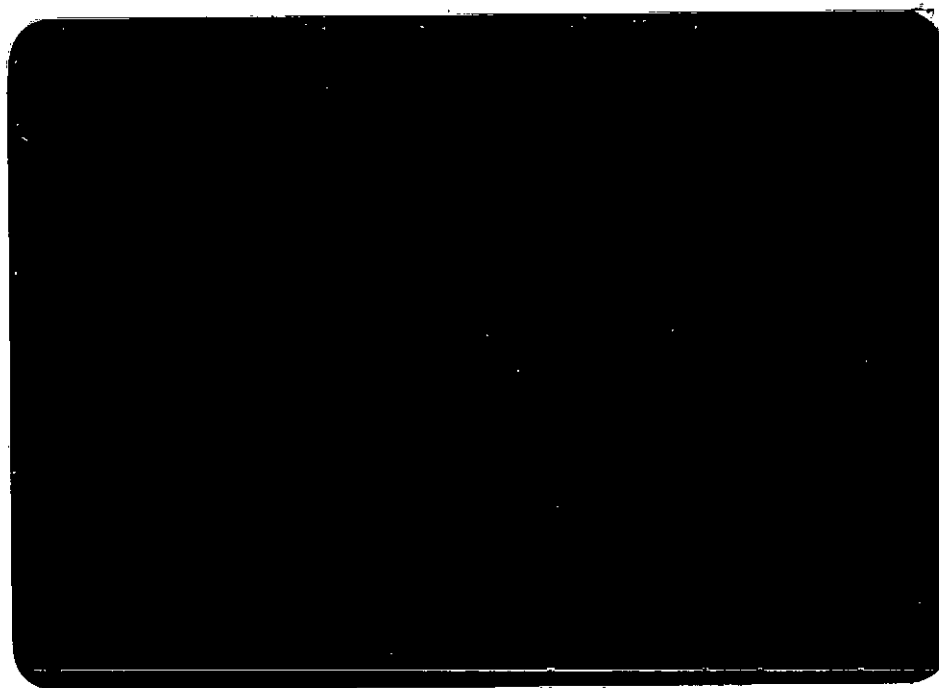
hours

Fig 5.7d   Mesophase mosaic formation developed on heat-treatment at 445^{0}C

for 5 hours

TABLE-1 (Row)

No. of obs.	2θ in degree	θ in degree	$d=\lambda/2\sin\theta$ in A
1.	10.25	5.125	8.619
2.	11.25	5.625	7.856
3.	14.55	7.275	6.081
4.	15.90	7.950	5.567
5.	17.70	8.850	5.005
6.	19.80	9.900	4.479
7.	20.80	10.400	4.265
8.	22.90	11.450	3.879
9.	24.20	12.100	3.673
10.	26.10	13.050	3.410
11.	27.30	13.650	3.263
12.	28.00	14.000	3.183
13.	31.40	15.700	2.846
14.	32.55	16.275	2.746
15.	44.10	22.500	2.051
16.	47.40	23.700	1.916

TABLE-2 $(410^0 C/2Hrs.)$

No. of obs.	2θ in degree	θ in degree	$d=\lambda/2\sin\theta$ in A
1.	10.30	5.15	8.578
2.	11.30	5.65	7.821
3.	14.60	7.30	6.059
4.	15.90	7.95	5.567
5.	17.70	8.85	5.005
6.	19.80	9.90	4.479
7.	20.80	10.40	4.265
8.	22.90	11.45	3.879
9.	24.20	12.10	3.673
10.	26.20	13.10	3.397
11.	28.00	14.00	3.188
12.	31.40	15.70	2.846
13.	32.40	16.20	2.759
14.	43.80	21.90	2.064
15.	47.20	23.60	1.923

TABLE-3 (410⁰C/4Hrs.)

No. of obs.	2θ in degree	θ in degree	$d = \lambda/2\sin\theta$ in A
1.	10.40	5.20	8.496
2.	11.40	5.70	7.753
3.	14.70	7.35	6.019
4.	16.10	8.50	5.209
5.	18.00	9.00	4.922
6.	20.20	10.10	4.391
7.	23.20	11.60	3.829
8.	24.40	12.20	3.644
9.	26.40	13.2	3.372
10.	28.30	14.150	3.149
11.	32.80	16.40	2.727
12.	44.80	22.40	2.021
13.	47.70	23.85	1.904

TABLE-4 (410^{0}C/6Hrs.)

No. of obs.	2θ in degree	θ in degree	d=λ/2sinθ in A
1.	10.50	5.25	8.415
2.	11.50	5.75	7.686
3.	14.90	7.45	5.939
4.	16.40	8.20	5.359
5.	18.00	9.00	4.922
6.	21.20	10.60	4.186
7.	23.30	11.65	3.813
8.	24.60	12.30	3.615
9.	26.50	13.25	3.359
10.	28.30	14.30	3.117
11.	33.10	16.55	2.703
12.	44.50	22.25	2.034
13.	47.90	23.95	1.897

TABLE-5 (440^0C/6Hrs.)

No. of obs.	2θ in degree	θ in degree	$d=\lambda/2\sin\theta$ in A
1.	10.55	5.275	8.375
2.	11.55	5.775	7.652
3.	14.85	7.425	5.958
4.	16.25	8.125	5.448
5.	18.15	9.075	4.882
6.	20.25	10.125	4.380
7.	23.25	11.625	3.821
8.	24.65	12.325	3.607
9.	26.55	13.275	3.353
10.	28.25	14.125	3.155
11.	44.35	22.175	2.040

TABLE-6 (470^{0}C/6Hrs.)

No. of obs.	2θ in degree	θ in degree	d=λ/2sinθ in A
1.	10.60	5.30	8.336
2.	11.60	5.80	7.620
3.	14.90	7.45	5.938
4.	16.30	8.15	5.432
5.	18.20	9.10	4.869
6.	20.30	10.15	4.369
7.	21.30	10.65	4.166
8.	23.30	11.65	3.813
9.	24.60	12.30	3.615
10.	26.60	13.3	3.347
11.	28.40	14.20	3.139
12.	33.00	16.50	2.711
13.	44.40	22.20	2.038

TABLE-7 Percentage of carbon yield

Sample No.	Temperature in ^{0}C	HT duration in Hrs.	Quantity of pyrene (gms)	Carbon yield (gms)	% of carbon yield
1.	500	4	0.5	0.40	80
2.		6	0.5	0.45	90
3.		8	0.5	0.47	94

TABLE-8 Rate of decrease of 'd' spacing with temperature

Sample	Temperature	HT duration	'd' spacing in A	Rate of change of 'd'/^{0}C
Anthracene	500^{0}C	2	3.440	0.0001
	600^{0}C	2	3.430	
Pyrene	500^{0}C	2	3.359	0.00012
	600^{0}C	2	3.347	

TABLE-9   Mesophase intervals in different aromatic samples

Sample	HT duration in Hrs.	Mesophase interval in ^{0}C
Anthracene	5	450-475=25
Phenanthrene	5	530-550=20
Pyrene	5	430-445=15

REFERENCES

5.1   Silverstein, R. M., Bassler, G. C., and Morril, T. C., Spectrometric Identification of Organic Compounds, John Willey & Sons. NY, 1981.

5.2   Robeot, T. C., Ifrared Spectroscopy, second Edition, 1975.

5.3   Conley, R. T., Infrared Spectroscopy, Allyn Bacon, London, second Edition, 1975.

5.4   Islam, O., Bhuiyan, A. H., and Ahmed, S., Thin Solid Films, 238, 191-194, 1994.

5.5   Farmer, V. C., The Infrared Spectra of Mnerals, Mineralogical Society, London, 1974.

5.6   Lapina, N. A., Ostrovskii, V.S., and Kamenskii, I. V., Vysokomol Soyed., AII, 2073, 1969 (Translated in Polymer Science USSR, 11, 2367, 1969.

5.7   Oberlin, A., Carbon, 22, 521, 1984.

5.8   Yagishita, H., Differential Thermal Analysis of Coals Misc. Rep. Res. Ins. Nat. Resour. Tokyo, 26, 40, 1952.

5.9   Brooks, J. D., and Taylor, G. H., Nature, 206, 697, 1965.

5.10   Singer, L. S., J. Chim. Phys., April, Sp. Vol. 21, 1969.

5.11   Rashid, M. A., Hossain, T. and Asgar, M.A., Thermochimica Acta, 259, 263-268, 1995.

5.12   Honda, H., Kimura, H., and Sanada, T., Carbon, 9, 695, 1971.

5.13   Kovac, C. A. and Lewis, I. C., Carbon, 16, 433, 1978.

5.14   Overlin, A., Carbon, 22(6), 521, 1984.

5.15   Kinney et al., Ind. and Eng. Chem., 49, 880, 1957.

5.16   Hossain, T., and Dollimore, J., Thermochimica Acta, 108, 211, 1986.

5.17   Jahan, S. T., and Hossain, T., Phy. Tea., Indian Phy. Soc., 2, 101, 1987.

5.18   Honda, H., Carbon, 26(2), 139, 1988.

5.19   Hossain, T., and Podder, J., Thermochimica Acta, 137, 225, 1989.

5.20   Jahan, S. T., M. Phil. Thesis, 1986.

5.21   Podder, J. , M. Phil. Thesis, 1986.

CHAPTER VI   CONCLUSIONS

6.1 Conclusions

6.1 CONCLUSIONS

The criteria of a graphitizable organic compound are summarized as follows:

1) In IR, the aromatic band at 900-575 cm^{-1} should have a higher intensity signifying the higher aromaticity of the sample.

2) For graphitizable organic materials, endothermal peaks should occur in the initial stage of the DTA trace.

3) Dynamic weight loss of the sample are to be found with the increase of temperature which are generally seen in TGA curves. Weight loss decrease with the progresses of carbonization as well as with the higher degree of graphitizability.

4) The inter-layer spacing in graphite structure is 3.354 A. In the graphitic carbons the apparent interlayer spacing should decrease with increasing temperature.

5) Organic materials which ultimately give rise to graphitizing carbons pass through a carbonaceous mesophase formation accompanied by temporary liquefaction or plasticising of the materials in the temperature range 350°C-600°C. In this liquid-state structural transition large lamellar molecules developed by the pyrolysis reaction become aligned in a parallel array to form an optically anisotropic liquid crystal. The mesophase spherules, the bulk mesophase and also the plastic flow patterns are formed during the relatively short life time of the carbonaceous mesophase as a prerequisite to graphitization.

IR spectra [Fig 5.1] clearly shows that all the absorption bands arises at the same region but intensity of the peaks decreases with increasing temperature. This is an indication of the modification to the pyrene structure on heat treatment. And also peaks at the 900-675 cm^{-1} band shows the higher intensities. It also shows higher aromaticity as well as higher graphitizability of pyrene.

DTA traces obtained for the compound under study (Fig 5.2) clearly indicate that endothermal processes of decomposition in the initial positions of the DTA curves of pyrene are typical like in all graphitizable organic materials.

TGA curves (Fig 5.3) shows that the carbon yield is increased with the increasing pyrolysis temperature (~50% carbon at 300°C). At a still more higher temperature at about 500°C the yield is found to be about 90% (Table 7). These results indicate that the pyrene is a highly graphitizable compared with other lower aromatic ring compounds.

X-ray spectra (Fig 5.4) reveals that, with the increasing carbonization, the interplanar spacing of carbon hexagonal planes decreases and approaches a regular crystalline structure as that of graphite. The relative decrease of interlayer spacing in the case of pyrene with increasing temperature and duration compared with other lower aromatic ring compounds under similar conditions indicates about the increasing degree of graphitizability in the case of pyrene.

The polarized-light photomicrographs (plate 5.7a-5.7e) obtained for the pyrene at different heat-treatment temperatures and durations clearly shows that it satisfies the 5th criteria of the graphitizable organic compounds, i.e., the compound passes through the carbonaceous mesophase transformation fulfilling the general features of a mesophase and hence it is graphitizable. The shortening of the mesophase interval again indicates that the degree of graphitization is higher compared with lower aromatic compounds.

REFERENCES

6.1   Islam, O., Bhuiyan, A. H. and Ahmed, S., Thin Solid Films, <u>238</u>, 191-194, 1994.

6.2   Bacon, G. E., Acta Crystal, <u>3</u>, 137, 1950.

6.3   Rooksby, H. P., Electric times, <u>102</u>, 19, 1942.

6.4   Gray, G. W., Molecular Structure and the Properties of Liquid Crystals, Academic Press, 1962.

6.5   Rashid, M. A., Hossain, T. and Asgar, M. A., Thermochimica, Acta, <u>159</u>, 263-268, 1995.

6.6   White, J. L., Guthrie, G. L. and Gardner, J. O., Carbon, <u>5</u>, 517, 1967.

6.7   White, J. L., Dubois, J. and Souillart, C., J. Chim. Phy. Special volume, April, 1969, 33; Euration report 4094e, 1969.

6.8   Dubois, J., Agace, C. and White, J. L., Euratom report, 4627e, 1971.

6.9   Honda, H., Kimura, H. and Sanada, Y, Carbon, <u>9</u>, 695, 1971.

6.10   Taylor, G. H., Fuel, <u>40</u>, 465, 1961.

6.11   Schmidt, W. J., Hondbuck der Mikroskopie in der Technik, <u>1</u>:1, 147, Verlag Umshaw (Ed. H. Freund): Frankfurt, 1957.

6.12   Brooks, J. D. and Taylor, G. H., Carbon, <u>3</u>, 185, 1965.

6.13   Kovac, C. A. and Lewis, I. C., Carbon, <u>16</u>, 433, 1978.

6.14   Hossain, T. and Dollimore, J., Thermochimica, Acta, <u>108</u>, 211, 1986.

6.15   Jahan, S. T. and Hossain, T., Phy. Tea., Indian Phy. Soc., <u>2</u>, 101, 1987.

6.16   Hossain, T. and Podder, J., Thermochimica, Acta, <u>137</u>, 225, 1989.